

NASA CR-174,961

DOE/NASA/0290-1  
NASA CR-174961

NASA-CR-174961  
19860005257

# Combustor Flame Flashback

Margaret P. Proctor and James S. T'ien  
Case Western Reserve University

LIBRARY COPY

DEC 23 1985

LIBRARY  
NATIONAL AERONAUTICS AND SPACE ADMINISTRATION  
HAMPTON, VIRGINIA

June 1985

Prepared for  
NATIONAL AERONAUTICS AND SPACE ADMINISTRATION  
Lewis Research Center  
Under Grant NAG 3-290

for  
**U.S. DEPARTMENT OF ENERGY**  
**Conservation and Renewable Energy**  
**Office of Vehicle and Engine R&D**



NF01227

## DISCLAIMER

This report was prepared as an account of work sponsored by an agency of the United States Government. Neither the United States Government nor any agency thereof, nor any of their employees, makes any warranty, express or implied, or assumes any legal liability or responsibility for the accuracy, completeness, or usefulness of any information, apparatus, product, or process disclosed, or represents that its use would not infringe privately owned rights. Reference herein to any specific commercial product, process, or service by trade name, trademark, manufacturer, or otherwise, does not necessarily constitute or imply its endorsement, recommendation, or favoring by the United States Government or any agency thereof. The views and opinions of authors expressed herein do not necessarily state or reflect those of the United States Government or any agency thereof.

Printed in the United States of America

Available from

National Technical Information Service  
U S Department of Commerce  
5285 Port Royal Road  
Springfield, VA 22161

NTIS price codes<sup>1</sup>

Printed copy A05  
Microfiche copy A01

<sup>1</sup>Codes are used for pricing all publications. The code is determined by the number of pages in the publication. Information pertaining to the pricing codes can be found in the current issues of the following publications, which are generally available in most libraries: *Energy Research Abstracts (ERA)*, *Government Reports Announcements and Index (GRA and I)*, *Scientific and Technical Abstract Reports (STAR)*, and publication, NTIS-PR-360 available from NTIS at the above address.

DOE/NASA/0290-1  
NASA CR-174961

## **Combustor Flame Flashback**

Margaret P. Proctor and James S. T'ien  
Case Western Reserve University  
Cleveland, Ohio

June 1985

Prepared for  
NATIONAL AERONAUTICS AND SPACE ADMINISTRATION  
Lewis Research Center  
Cleveland, Ohio 44135  
Under Grant NAG 3-290

for  
U.S. DEPARTMENT OF ENERGY  
Conservation and Renewable Energy  
Office of Vehicle and Engine R&D  
Washington, D.C. 20545  
Under Interagency Agreement DE-AI01-77CS51040

## TABLE OF CONTENTS

	Page
CHAPTER I INTRODUCTION	1
I.1 Motivation	1
I.2 Literature Survey	1
I.3 The Present Study	4
CHAPTER II EXPERIMENTAL APPARATUS	6
II.1 Facility	6
II.2 Test Section	6
II.3 Instrumentation	9
II.4 Data Aquisition and Analysis	11
CHAPTER III. PROCEDURI:	13
CHAPTER IV. EXPERIMENTAL RESULTS AND DISCUS- SION	14
IV.1 Visual Observations	14
IV.2 Verification of Flashback	15
IV.3 Gas Analysis Data	16
IV.4 Parametric Study	17
IV.5 Pressure Oscillations	20
IV.6 Flow Reversals	22
CHAPTER V. ANALYSIS OF FLOW REVERSAL IN PREMIXING CHANNELS	24
V.1 Relevance	24
V.2 Flow Reversal Model	25
V.3 Governing Equation and Solution	27
V.4 Values of Nondimensional Parameters	30
V.5 Critical Pressure Gradients Ratio for Flow Reversal	33
V.6 Velocity Profiles Near the Wall	34
V.7 Flame Flashback in Oscillatory Flow	36
V.8 Status of Modeling Periodic Turbulent Flow in Pipes	38
CHAPTER VI CONCLUSIONS AND REOCMMENDATIONS	40
LIST OF REFERENCES	43

## CHAPTER I

### INTRODUCTION

#### 1.1. *Motivation*

Premixed-prevaporized combustors operate with uniformly lean fuel/air ratios and consequently produce lower emission levels of  $NO_x$  and soot than diffusion flame combustors. For this reason, they are candidates for advanced automotive and aircraft gas turbines. Flashback, a problem that occurs in premixed-prevaporized combustors, is the upstream propagation of the flame from the combustor into the premixing tube. Not only does flashback change the combustion process from premixed burning to diffusion burning, thus creating more pollutants, but it also inflicts considerable damage on the fuel injector, premixing tube and other equipment upstream. Therefore, before implementing the premixed combustor, an understanding of the flashback mechanisms should be achieved and a scheme for preventing its occurrence has to be found.

#### 1.2. *Literature Survey*

A reasonable number of studies on flame flashback in a bunsen burner have been done (see Lewis and von Elbe (1961), for example). With this device a premixed flame was first established at the mouth of the tube. Flashback was then induced by gradually decreasing the mixture flow rate. The experiments were normally

conducted in steady-state and laminar flow conditions. From experimental data, Lewis and von Elbe (1961) established a velocity gradient criterion based on the velocity balance concept. Simply stated, flashback will occur when the mixture velocity gradient at the wall becomes small enough that the local mixture velocity at the edge of the wall quenching layer is less than the flame speed. Lewis and von Elbe were able to correlate a number of flashback data using this criterion. Further work along a similar line was done by Putnam and Jensen (1949) who utilized a Peclet number correlation.

Despite these earlier efforts, a more fundamental analysis has not appeared until recently. Lee and T'ien (1982) formulated and solved the laminar flame flashback problem in a circular tube using two-dimensional Navier-Stokes' conservation equations. This more basic approach can handle more complicated situations such as non-linear velocity profiles and unequal mixture and wall temperatures. In addition, the computation provides detailed flame structure at the flashback limit without making any ad hoc assumptions about quenching distance.

The investigations above were for steady-state. Since the laminar flame speeds for most hydrocarbon/air mixtures are rather low (of the order of 1 m/s or less), in a laminar flow this "classical flashback mode" can only occur when the mixture velocity is low and the boundary layer is relatively thick.

In comparison, flashback in a premixed flame combustor is far more complicated. First, the flow is turbulent; turbulent flame speeds can be much higher than laminar ones. Also, turbulent boundary layers are thinner and quenching distances are smaller because of higher pressures and wall temperatures. Second, because the combustor is partially enclosed, a mechanism of gas dynamic coupling exists. In other words, a disturbance in the combustor can affect the flow in the premixer and vice versa. Therefore, consideration of transient conditions are necessary.

Since interest in premixed-prevaporized combustors is relatively recent, intentional investigations of combustor flashback are very few. Most reported "flashbacks" occurred when experimenters were investigating something else. Plee and Mellor (1978) examined twenty-one cases of reported flame stabilization in the fuel-preparation tube. Because the interiors of these combustors were not optically accessible, the upstream flame stabilizations were discovered by either burnt out parts, thermocouple readings in the premixer or a change of emission levels. The reasons why the flame stabilized in the premixer had to be inferred from the design of each apparatus rather than from direct observations or measurements. Plee and Mellor (1978) felt the classical flashback mode was unlikely in most cases because mixture velocities were too great. They concluded that some upstream stabilizations occurred as a result of flow separation behind consecutive steps or bluff bodies and in other cases as a result of autoignition. However, these authors did not

consider transient mechanisms.

Coats (1980). In a comment to the review by Plee and Mellor, mentioned that flashback and combustion instability have been observed to occur simultaneously. In a separate experiment at ambient conditions using a transparent window on the sidewall of the combustor, Ganji and Sawyer (1979) observed a flickering type flame flashback in concurrence with combustor pressure oscillations. In the flickering mode, the flame, in a periodic manner, moved upstream past the flame stabilization hump into the premixing channel and then retreated back into the combustor. In a further study using the same setup, Keller et al (1981) identified several combustion pressure oscillation modes prior to the induced flashback and used Schlieren cinematography to study the flame movement. It was noticed that during the upstream flickering motion, the leading edge of the flame front was always close to the wall. Thus, a transient boundary layer flow retardation or reversal may have been present and may be responsible for the flame flickering motion [see Plee and Mellor (1980)].

### *1.3. The Present Study*

The above discussion illustrates the complicated nature of combustor flashback phenomena and the lack of information associated with them. For example, it is not clear whether the concurrent appearance of instability and flashback is geometrically specific as suggested by Coats or more general in nature. There has been no systematic investigation of flashback over a range of velocities and at

high mixture and premixer wall temperatures.

The objective of the present study was to investigate flashback under controlled conditions simulating gas turbine combustor operations to identify flashback regimes under steady-state and transient conditions. A premixed-prevaporized, rectangular, center-dump combustor with quartz window sidewalls for visual access was designed, constructed and tested. The 1 in. high and 4 in. wide premixer dumped into the 4 in. by 4 in. combustor. Gaseous propane and air were burned. A parametric study was done to determine the effects of inlet air temperature in the range of 600 to 850 K, premixer wall temperature in the range of 450 to 900 K, and average premixer velocity in the range of 40 to 80 ft/s on the fuel/air equivalence ratio required for flashback. High speed photography and high frequency response pressure transducers were used to investigate the mechanism of flashback. Finally, a theoretical analysis was performed for periodic flow in the premixer in order to assess the effect of pressure oscillation on flame flashback.

## CHAPTER II

### EXPERIMENTAL APPARATUS

#### *II.1. Facility*

The test section was installed at NASA Lewis Research Center in cell 11B of the Combustion Research Laboratory. Operation of the test combustor was done from the control room where conditions were monitored and data recorded. Photographs of the control room and the test section installed in the facility can be found in Ref. 12. The existing propane, air, water and steam systems were employed with a few changes in orifice and valve sizes. Schematics of these are also in Ref. 12.

#### *II.2. Test Section*

The test section, shown in figures 1 and 2, was a stainless steel, rectangular, premixed-prevaporized, center-dump combustor. It was designed to two-dimensionalize the experiment (rectangular cross section), provide visual access to the combustion process, withstand five atmospheres pressure, and operate at conditions similar to those of automotive gas turbines.

Non-vitiated preheated air from the facility's natural-gas-fired preheater was supplied to the premixing tube through a 47 in. long, insulated transition section with an inside cross section 3.5 in. wide and 1.0 in. high. This length (approximately 30 hydraulic flame-

ters) assured a fully-developed velocity profile at the entrance of the premixing tube.

The fuel injector, figure 3, was a 1/4 in. outside diameter, 0.035 in. thick wall stainless steel tube with eight 0.02 in. diameter holes evenly spaced along its length. It was mounted horizontally in the transition section 8 in. upstream of the step with the holes facing the downstream direction. Gaseous propane was supplied to both ends of the fuel injector. A small portion of data was taken with the fuel injector 25 1/2 in. upstream of the step to determine the effect of mixing length and to verify the location of upstream flame stabilization.

The propane and air from the transition section mixed in the premixing tube, 6 1/2 in. long, 1 in. high and 4 in. wide, before dumping into the 4 in. by 4 in., 10 1/2 in. long combustion chamber. At the sudden expansion, recirculation zones formed behind the two symmetric 1 1/2 in. steps to stabilize the flame. The temperature of the premixing tube walls was adjusted by passing air through an insulated channel adjacent to each wall. This air either cooled or heated the wall depending on the setting of two 5 kw electric heaters through which it passed. A 15-joule electric spark igniter, flush mounted in the top combustor wall 3 3/4 in. downstream of the step, was used to initiate combustion. The igniter fired for 30 seconds. If sustained combustion was not attained within that time the propane trailer valve closed automatically to prevent propane buildup in the system.

Combustion products entered the exhaust plenum through a 2.0 in. diameter hole (see Fig. 1a). The exhaust plenum, a stainless steel box, supported a conical plunger and the two solenoids which moved it. A switch in the control room enabled the solenoids, pushing the plunger partially into the 2.0 in. diameter hole to create either a pulsed or sustained pressure increase. Although use of the plunger to create transient conditions was intended, no testing was done with it in this study. The plunger cooling water dumped into the exhaust plenum to cool the hot gases and to protect the exhaust pipes and muffler (see figure 1a).

Two 1/2 in. thick, 5 in. by 16 in. optical quality quartz windows formed the sidewalls of the test section and provided visual access to the entire combustion process. Early in the testing, one quartz window was replaced with a stainless steel plate which provided a better background for viewing the flame. High temperature gasket material placed between the combustor sidewall and the window formed a 1/16 in. gap above and below the premixing tube (see figure 1c). The upper and lower edges of the window gasket were unconfined and often blew out when rig pressure was raised to approximately 20 psia to take gas emissions data.

After warped window flanges resulted in the breaking of several quartz windows, both windows were replaced by stainless steel plates. Flashback, previously detected visually, was then detected by a chromel-alumel thermocouple mounted in one of the stainless steel plates, 1 in. upstream of the step, centered in the

premixing tube 1/8 in. away from the sidewall. The 0.020 in. diameter wires were joined by a 1/16 in. bead. The final tests were made with a 6 in. diameter quartz window machined to mount flush in one of the stainless steel plates as shown in figure 4.

### II.3. Instrumentation

Temperature. Average premixer and combustor wall temperatures were measured with chromel-alumel thermocouples embedded in the top and bottom walls. Open ball platinum-rhodium thermocouples extending 1/2 in. from the combustor wall into the combustion zone measured gas temperatures. The locations of these thermocouples are shown in figures 5 and 6. A matrix of chromel-alumel thermocouples mounted in the transition section just upstream of the fuel injector, as shown in figure 7, measured the inlet air temperature. All thermocouples had 1/16 in. beads. The temperature of the propane-air mixture was estimated to be between 94 and 98 percent of the inlet air temperature at operating conditions.

Pressure. The inlet and combustor pressures were measured at locations shown in figures 7 and 5. Observation of small pressure oscillations was facilitated by the use of 2.0 psig Endevco piezoelectric transducers with a 45,000 Hz resonance frequency. A limited amount of data was taken with the inlet transducer at an alternate location, 41.25 in. upstream of the step, to examine the phase relation between the two transducers.

Flowrates. Flowrates were measured with orifice runs. The pipe and orifice diameters used to measure the flowrates of combustion air, propane, and wall heating air are presented in Table 1.

Table 1. Orifice and Pipe Diameters

Gas	Pipe Diameter (Inches)	Orifice Diameter (Inches)
Combustion air	2.0	0.4003
Propane	0.5 (tube)	0.05
Wall heating air	0.75	0.15

The upstream pressure and the pressure drop across the orifice were measured with 200 psia and 50 psid transducers, respectively. Chromel-alumel thermocouples measured upstream orifice temperatures. To insure the gaseous state of propane at its orifice an upstream pressure of 150 psia and a temperature of at least 180°F was maintained. A 0.10 gal/min turbine meter was installed in the propane system to verify the orifice measurements. Once verification was made, use of the turbine meter was discontinued.

Exhaust Emissions. Emission measurements were occasionally made to check the uniformity of the fuel/air profile. Exhaust emissions of  $NO_x$ , CO,  $CO_2$  and unburned hydrocarbons were measured with the facility gas analyzer. To take emissions data the rig pressure was raised to approximately 20 psia, by partially closing the

exhaust valve, to force the sample into the gas analyzer probe and to achieve a sufficient sample flowrate to the analyzer. The probe was water cooled to rapidly quench the reactions in the sample and the sample line was heated to 350°F to prevent condensation of hydrocarbons. Located near the exit of the combustor (figure 6), the probe was mounted on an L.C. Smith controller to traverse to several vertical locations in the combustor. Concentrations of carbon monoxide and carbon dioxide were measured with nondispersive infrared analyzers, total nitrogen oxides ( $NO$  and  $NO_2$ ) with a chemiluminescent analyzer and unburned hydrocarbons with a flame ionization detector.

#### *II.4. Data Acquisition and Analysis*

Several systems were used for data acquisition. The bulk of the data was taken via Escort II, a dedicated PDP-11 mini-computer. Raw data (millivolts) from the instrumentation was fed to Escort II. In the normal running mode, Escort II displayed various parameters, such as flowrates and temperatures which were calculated from raw data, on a CRT screen. The display was updated every 2 seconds. When data were recorded by manually pushing the "record" button, the raw millivolt data were stored on a legal record tape and transmitted to the IBM 370 computer's data collector where it was stored in the proper data set for further calculations and analysis. Certain calculated values were stored in a separate data set for each reading to facilitate plotting data via the post-test interactive graphics package. Selected calculations can be found in

Ref. 12.

An 8 channel strip chart recorder was used to monitor pressures in the inlet and combustor, and the flashback thermocouple temperature. Inlet and combustor pressures were also recorded on a Bascom-Turner digital data recorder for a few test runs. Data were recorded every 100  $\mu$ s for 150 ms and stored on an 8 in. floppy disk. Data could then be played back to a plotter with adjusted scales for maximum readability.

Visual observations were recorded by a video camera in conjunction with a Sony Beta Max video recorder. Most tests run with visual access were taped. Several 16 mm. high speed movie cameras, including a Milliken DPM 55, a Hycam II and a Fastax WF3, were used to film flashback at 200, 400 and 1000 frames/sec.

## CHAPTER III

### PROCEDURE

The following procedure was followed in collecting flashback data:

1. The inlet air temperature, premixer wall temperature, and average premixer velocity were adjusted to the desired values.
2. The video and brush recorders were turned on.
3. The igniter was started and the fuel was permitted to flow to the test section initiating combustion at the step.
4. After the igniter timed out, the fuel/air equivalence ratio was increased (by increasing the fuel flowrate) until flashback occurred at which time data was recorded. Visual observation of the flame and/or the trace of the flashback thermocouple on the brush recorder monitored the occurrence of flashback.

The test conditions were as follows: inlet air temperature, 600 to 850 K; premixer wall temperature, 450 to 900 K; premixing tube velocity, 40 to 80 ft/s, equivalence ratio, up to 0.8.

## CHAPTER IV

### EXPERIMENTAL RESULTS AND DISCUSSION

#### IV.1. *Visual Observation*

As the fuel/air equivalence ratio was increased to the point of flashback, several stages of burning were observed. Photographs from a video tape of an early test run with a 5 X 16 in. quartz window illustrate these stages and are shown in figure 8. Flow is from right to left with the premixer on the right dumping into the combustor on the left. The bright spots near the combustor walls are thermocouples. Test conditions were: inlet air temperature, 850 K; premixer wall temperature, 750 K; average premixer velocity 70 ft/s. Photographs a-e are in order of increasing equivalence ratio,  $\phi$ , with the exception that (a) and (b) have approximately the same equivalence ratio. A very lean flame ( $\phi=0.41$ ) attaches to the lower step (a) or in some cases attaches to both steps (b), occasionally moving downstream as though it is about to blow off. At increased equivalence ratio ( $\phi=0.44$ ) the flame attaches to both steps with strong recirculation zones becoming visible behind them as seen in (c). A further increase in equivalence ratio to 0.56 causes the flame to flicker (sporadic extension of the flame front in and out of the premixing tube). Figure 8(d) shows the flame front just upstream of the step as flickering begins. The distance of flame propagation during flickering increases with equivalence ratio

( $\phi=0.60$ ) until a maintained flashback is induced, stabilizing the flame in the premixing tube, (e). The data presented in this report were for maintained flashback. It is presumed the flame was stabilized by recirculation zones at the 0.25 in. steps formed by the premixer sidewalls and the quartz windows (see figures 1b and 1c for location of 1/4 in. steps). This is substantiated by the location of the flame front downstream of the 0.25 in. steps as shown in figure 9.

#### IV.2. *Verification of Flashback*

Two tests were conducted to verify that the phenomenon observed was flashback and not autoignition. First, at the conditions most conducive to autoignition within the operating range, gaseous propane was permitted to flow to the test section without firing the igniter for 30 seconds. An equivalence ratio up to 1.2 was obtained at an inlet air temperature of 846K, premixer wall temperature of 701 K and average premixer velocity of 38 ft/s without autoignition occurring.

Second, flashback was filmed with high speed photography. The sequence of photographs in figure 10, taken at 400 frames/s, confirms the upstream flame propagation from the combustor into the premixer. Initial test conditions were: inlet air temperature, 830 K; premixer wall temperature, 750 K; average premixer velocity, 86 ft/s. For filming purposes flashback was induced by decreasing the premixer velocity to 76 ft/s. The equivalence ratio at maintained flashback was 0.48. The first photograph, (a), shows the step

location. Flow is from right to left. Visual access was through a 6.0 in. diameter window mounted in a stainless steel plate. In frame (b) the flame is strongly attached to the lower step. The next frame, (c), shows the flame attached to the upper step just inside the premixing tube. The flame in (d) has propagated upstream with the leading edge along the top premixer wall. Frames (e) and (f) show the flame front gaining distance upstream, but dimming in brightness. In frame (g) the flame front has retreated with the leading edge on the centerline and become brighter. In frames (h) through (k) the flame continues its upstream propagation until it is stabilized in the premixing tube as seen in frame (l). This sequence of frames further verifies the occurrence of flashback.

#### IV.3. Gas Analysis Data

Exhaust gas emissions samples were taken near the exit of the combustor at several vertical locations by traversing a gas sampling probe. Analysis of the exhaust sample yielded  $CO$ ,  $CO_2$ ,  $NO_x$  and  $HC$  concentrations from which the equivalence ratio was calculated [anonymous (1980)]. This equivalence ratio was compared to that calculated from fuel and air flowrates. A profile of the ratio of these two equivalence ratios is shown in figure 11. The two methods of measurements agree within  $\pm 10$  percent; the profile across the combustor is fairly uniform. The combustion efficiency was always approximately 99 percent.

#### IV.4. *Parametric Study*

A parametric study was done to determine the effects of inlet air temperature, premixer wall temperature, premixing tube velocity and fuel injector location on the minimum equivalence ratio required for a maintained flashback. Each plotted data point represents a single set of maintained flashback conditions. Thus the data plots show the actual data scatter.

The inlet air temperature effect is slight as shown in figure 12. The equivalence ratio at which maintained flashback occurred is plotted against inlet air temperature. As inlet air temperature increases the equivalence ratio decreases as expected. At premixer velocity of 60 ft/s the equivalence ratio at maintained flashback decreases from .68 at an inlet air temperature of 600 K to .5 at an inlet temperature of 850 K. This trend occurs at premixer velocities of 40, 50 and 60 ft/s. Note that the equivalence ratio for maintained flashback is lower at a premixer velocity of 60 ft/s than at 40 ft/s.

The effects of premixer wall temperature and premixing tube velocity are unclear. Figure 13 illustrates the relation of the maintained flashback equivalence ratio to the average premixing tube velocity at an inlet air temperature of 600 K at six different premixer wall temperatures. Data scatter is such that separate curves for each premixer wall temperature are indistinguishable. Thus, the effect of the premixer wall temperature on the flashback equivalence ratio is unclear.

Originally, it was thought that flame flashback might be caused in the wall boundary layer by the velocity balance mechanism [Lewis and von Elbe (1961)] because of the high wall temperatures. According to the velocity balance concept in steady-state, flashback can occur if the flame speed at the edge of the wall quenching layer exceeds the local flow velocity. The data in figures 12 and 13, however, do not support this mechanism. Flashback occurred at lower equivalence ratios as the premixer velocity was increased. (A decrease in equivalence ratio decreases flame speed.) Clearly, this trend opposes the steady-state velocity balance concept. Furthermore, if flashback were to be explained by this concept, one would expect that as wall temperature was increased, flashback would occur at lower equivalence ratios. Fig. 13 shows that such a trend did not occur in the present tests. When wall temperature was increased from 500 to 700K, there was no evident change in flashback equivalence ratio.

The data discussed so far were taken with the fuel injector mounted 8 in. upstream of the step. A small portion of data were taken with the fuel injector 25 1/2 in. upstream of the step. This greater distance increased the amount of time for the propane and air to mix. Flashback equivalence ratios were the same, within data scatter, for both fuel injector locations.

At the 25-1/2 in. position the equivalence ratio at which flickering first began was also recorded. The magnitude of the difference between the flickering equivalence ratio and flashback

equivalence ratio is shown in figure 14 which is typical. However, in some cases the difference was almost negligible as in figure 15. In view of these results it should be emphasized that as the equivalence ratio was increased from a lean flame on the step, flickering always preceded flashback. It is interesting to note that figures 14 and 15 show a trend opposite of figures 12 and 13 of the maintained flashback equivalence ratio vs. average premixer velocity. This may suggest nonuniform mixing when the fuel injector was only 8 in. upstream of the step. The parametric data discussed are representative of a larger body of data. Data at other test conditions can be found in Ref. 12.

The amount of scatter in the data from the parametric study is disturbing. The error bars for premixer velocity, equivalence ratio, and inlet air temperature are shown in figures 12 and 13. The average premixer velocity was measured within  $\pm 2.0$  ft/s, the inlet air and premixer wall temperatures within  $\pm 10$  K, and the equivalence ratio within  $\pm 0.005$ . These error bars do not entirely account for the data scatter. It is suspected that the problem resulted from taking data at *maintained flashback*. To achieve maintained flashback, the flame had to stabilize in the 1/4 in. step in the premixer. Stabilization at such a small step may have been responsible for the randomness in the data. If the results were indeed dependent on the location and size of the upstream flame stabilization step, then they will not be generally valid, but are unique to the geometry studied.

#### IV.5. *Pressure Oscillations*

It was discovered that pressure oscillations were present in the premixing tube and combustor during combustion. The oscillations had a frequency of 40 to 80 cycles/s and a peak-to-peak amplitude of up to 1.4 psi. Similar oscillation frequencies and amplitudes were found by Keller (1981). As the equivalence ratio was increased from a lean flame at the step the peak-to-peak amplitude of the oscillations increased to some maximum value just before flashback occurred. Once the flame stabilized in the premixing tube the amplitude greatly decreased. Typical strip chart recordings of this observation are shown in figure 16. Only the combustor oscillations are presented in this figure. The premixer oscillations were very similar because the two transducers were only separated by 9 3/4 in. In figure 16, time advances from right to left as does the equivalence ratio. A fairly large increase of equivalence ratio occurred between  $\phi_1$  and  $\phi_3$ . However, a much smaller increase was required between  $\phi_3$  and  $\phi_4$ . The relationship between the peak-to-peak amplitude and the equivalence ratio is illustrated in figure 17. The same trend occurs at several velocities. It was also observed that frequency increased as either the premixing tube velocity or the equivalence ratio increased as shown in figure 18.

Since the scale of the strip charts was small and a phase difference between the premixer and combustor pressure oscillations was difficult if not impossible to detect, a digital data recorder was also used. The premixer pressure transducer was relocated 43.75

in. upstream of the combustor pressure transducer. It was hoped this would magnify any phase difference between the two transducers. A sampling interval of  $100 \mu\text{s}$  was used to give greater details of the oscillation shapes. Several recordings made at different equivalence ratios and stages of burning are shown in figure 19. Recording (a), taken while the flame was behind the dump plane shows low amplitude pressure oscillations. Pressure oscillations during flame flickering had a greater amplitude as shown in recording (b). The shape of the combustor pressure trace is more complex with a low peak followed by a high peak. During recording (c) the flame was still flickering but at a higher equivalence ratio. Again the oscillation amplitude increases with higher frequency components present in the inlet pressure trace. Recording (d) was taken while the flame was stabilized in the premixer. The amplitude is decreased and higher frequency components have become more apparent in both the premixer and combustor pressure traces.

Similar pressure recordings were made for a higher premixing tube velocity of 60 ft/s. Pressure traces of lean flames in the combustor and at the step are shown in figure 20(a) and (b). The amplitude during flickering, recordings (c) and (d), is significantly higher than those in figure 19 (possible explanation is offered in Chap. V). Also, double pressure peaks recorded in the inlet are not seen in the previous figures. Flickering continued as the equivalence ratio was increased further and the amplitude of the pressure oscillations increased further as is shown in recording (e).

Parts of the pressure traces of recordings (f) and (g) have decreased amplitudes characteristic of flame stabilization in the premixing tube and others have greater amplitudes like those of flickering. This is understandable as the flame was only momentarily stabilized in the premixing tube when these recordings were made. In all recordings there exists a phase shift between the combustor pressure and the inlet pressure peaks. However, the phase shift calculated using the speed of sound with a one-dimensional standing wave (see Ref. 12) did not agree entirely with the measured phase shift. For example, in one case the calculated phase shift was 37 degrees and the measured phase shift was 51 degrees. In another case the calculated phase shift was 43 degrees and the measured was 133 degrees. A more complicated analysis was not attempted.

#### IV.6. *Flow Reversals*

Although the peak-to-peak amplitude of the pressure oscillations was small (up to 1.0 psi), it would have been large enough to induce local flow reversals in the premixing tube since the pressure drop in the premixer is much smaller (see Chap. V for their estimates). A simple experiment was performed to determine if flow reversals did occur near the premixer exit. Ceramic fibers of high temperature gasket material were cemented with ceramic cement to the top and bottom premixer walls 1 in. upstream of the step, to the top and bottom combustor walls 1 in. downstream of the step, and to the vertical faces of the step. The ceramic fibers attached to the vertical faces of the step were blown upstream into the

premixing tube during flickering. Thus, flow reversals did occur near the premixer exit, however the magnitude and the extent of the reversals have not yet been determined experimentally. A theoretical analysis of flow reversal in the premixing channel is given in the next chapter.

## CHAPTER V

### ANALYSIS OF FLOW REVERSAL IN PREMIXING CHANNELS

#### V.1. *Relevance*

The last chapter on flame flashback experiments strongly suggests that flow reversal may occur during combustion oscillation and can be responsible for the observed flashback phenomenon. To substantiate this further, the following estimate is given. Fig. 18 indicates that at average premixer velocity of 40 ft/s, the pressure oscillation frequency is 48 Hz. The time for flame to flicker upstream is at most half of the oscillating period, i.e. 10.4 ms. At the instance the flame becomes anchored in the premixer, it has to travel 6 inches as indicated in Fig. 9. The average velocity for upstream flame motion is then at least 48 ft/s. This value is too great for flame burning velocity. Therefore a concurrent fluid flow must be with the flame motion as it approaches the fuel injector.

In order to obtain more understanding of the flow reversal phenomenon in the premixing channel, a fluid mechanical analysis is made based on a simplified model.

## V.2. *Flow Reversal Model*

The following assumptions are made:

1. The flow in the premixer is non-chemically reacting.
2. The flow in the premixer is two-dimensional.
3. The flow is fully-developed for both steady and oscillatory states.
4. The flow is incompressible and laminar.

Before we write down the governing equation for the flow, these assumptions will be discussed.

The non-chemically-reacting assumption is valid if the temperature in the premixer is not high enough to cause considerable heat release in the premixing channel; a condition which is satisfied in our experiments. It also restricts the application of our theoretical results to regions ahead of the flame when flashback occurs.

In the experiment, the premixing channel has a rectangular cross-section with aspect ratio of 4 to 1, so a two-dimensional approximation is adopted in the analysis.

The premixer has a long entrance section (entrance length to height ratio = 47), so the steady flow in the premixing section should be fully-developed. The same assumption for the oscillatory state requires explanation. The observed pressure oscillation frequencies are from 48 to 75 Hz. The corresponding quarter wave lengths are estimated to be from 9.5 to 6.1 feet based on an air temperature of 800 K. Since the premixing channel is only 6-1/2 inches long and it is the only section of interest to us, the pressure

distribution over this section can be taken approximately as linear. In other words, using this "long wave approximation", the pressure gradient is a constant over space in the premixer at any given instance during the oscillation, hence a fully-developed flow. Although the work fluid is gaseous, the incompressible flow assumption is valid because under the long wave approximation, no wave propagation phenomenon is involved. The flow is driven by pressure gradient alone and both the pressure differential and the velocity magnitude are small enough to justify the incompressible assumption.

The laminar flow assumption is perhaps the most uncertain. The Reynolds numbers based on the channel height are from 3800 to 7600 for average flow velocities from 40 to 80 ft/sec. According to the linear theory of hydrodynamic stability, the critical Reynolds number is 5772 for two-dimensional Poiseuille flow [Reshotko (1984)]. So if free stream turbulence can be avoided in the upstream, our flow can either be laminar or transitional (turbulent), depending on the operating Reynolds numbers. In reality, a disturbance-free upstream flow is difficult to achieve; the flows in our experiments are more likely to be turbulent. The use of laminar flow in our analysis can only be taken as the first step in the understanding of this complicated flow phenomena. a discussion of the status of modeling periodic turbulent pipe flow can be found later in Section V. 8.

### V.3. Governing Equation and Solution

With the above assumptions, the governing equation and boundary conditions for the flow are

$$\frac{\partial u}{\partial t} = -\frac{1}{\rho} \frac{\partial p}{\partial x} + \nu \frac{\partial^2 u}{\partial y^2} \quad (1)$$

$$u(y=0) = 0$$

$$u(y=h) = 0$$

Referring to Fig. 21,  $u$  is the fluid velocity along the channel direction  $x$  which is a function of  $y$  and  $t$ ; the pressure gradient  $\partial p/\partial x$  is a function of  $t$  only,  $h$  is the height of the channel and  $\nu$  is the kinematic viscosity of the fluid. The pressure gradient can be decomposed into steady and unsteady parts:

$$-\frac{1}{\rho} \frac{\partial p}{\partial x} = -\frac{1}{\rho} \frac{\partial \bar{p}}{\partial x} - \frac{1}{\rho} \frac{\partial p'}{\partial x} \quad (2)$$

The steady part of the pressure gradient is a constant and the unsteady part is assumed to be oscillatory given by the following expression:

$$-\frac{1}{\rho} \frac{\partial p'}{\partial x} = a \cos \omega t \quad (3)$$

where  $a$  is the amplitude of the pressure gradient oscillation and  $\omega$  is the oscillation frequency in radian/second.

Using Eqs. (2) and (3), Eq. (1) can be separated into steady and oscillatory equations as follows:

$$\frac{1}{\rho} \frac{\partial \bar{p}}{\partial x} = \nu \frac{\partial^2 \bar{u}}{\partial y^2} \quad (4)$$

$$\bar{u}(0) = \bar{u}(h) = 0$$

and

$$\frac{\partial u'}{\partial t} = a \cos \omega t + \nu \frac{\partial^2 u'}{\partial y^2} \quad (5)$$

$$u'(0, t) = u'(h, t) = 0$$

Here, we would like to emphasize that the separation into Eqs. (4) and (5) is due to the *linearity* of Eq. (1), there is no restriction on the magnitude of the oscillatory pressure gradient. As a matter of fact, we shall see later, the more interesting cases are those when oscillating amplitudes are much greater than the mean.

Eq. (4) is the well-known equation for two-dimensional Poiseuille flow. The solution is

$$\frac{\bar{u}}{u_m} = \frac{3}{2} \left[ 1 - \left[ \frac{2y}{h} - 1 \right]^2 \right] \quad (6)$$

the mean (average) velocity,  $u_m$ , is given by

$$u_m = \frac{h^2}{12\nu} \frac{1}{\rho} \frac{\partial \bar{p}}{\partial x} \quad (7)$$

Since Eq. (5) is linear, it can be solved more easily by using the complex variable notation, i. e.

$$\frac{\partial u'}{\partial t} = a e^{-i\omega t} + \nu \frac{\partial^2 u'}{\partial y^2}$$

The solution can be found in Landau and Lifshitz (1959):

$$u'/(a/\omega) = i e^{i\omega t} \left[ 1 - \frac{\cos \left\{ (1+i) \left[ \frac{y}{\delta} - \frac{h}{2\delta} \right] \right\}}{\cos \left\{ (1+i) \frac{h}{2\delta} \right\}} \right] \quad (8)$$

where

$$\delta = \sqrt{2\nu/\omega} \quad (9)$$

is the characteristic depth for the oscillatory flow.

Nondimensionalizing  $u'$  by  $u_m$ , we get

$$\frac{u'}{u_m} = \frac{3}{2} \left( \frac{2\delta}{h} \right)^2 r_p \frac{u'}{\left( \frac{a}{\omega} \right)} \quad (10)$$

where  $r_p = \left| \frac{\partial p'}{\partial x} \right| / \frac{\partial \bar{p}}{\partial x}$  is the ratio of the amplitude of the oscillatory-pressure gradient to the pressure gradient in the steady flow.

It should be noted that only the real part of Eq. (8) is relevant. The total flow velocity is the sum of the steady and the oscillatory parts, i. e.

$$\frac{u}{u_m} = \frac{\bar{u}}{u_m} + \frac{u'}{u_m} \quad (11)$$

From Eqs. (6), (8) and (10), we can see that

$$\frac{u}{u_m} \left[ \frac{2y}{h}, \omega t \right] = \text{function of} \quad \left[ \frac{h}{2\delta}, r_p \right]$$

In nondimensional form, the velocity depends only on two dimensionless parameters. They are the ratio of the half channel height to the characteristic oscillation depth and the ratio of the oscillatory pressure gradient amplitude to the steady-flow pressure gradient.

#### V.4. Values of Nondimensional Parameters

Before analyzing the details of the solution, the typical values of the two nondimensional parameters corresponding to the experimental conditions are listed in Tables 2 and 3.

Table 2. Ratio of Half Channel Height to Characteristic Oscillation Depth  
(for  $\theta = 0.47$ )

$U_m$	$\omega$	$\delta$	$h/2$	$h/2\delta$
ft/s	Hz	cm	cm	
40	48	0.0735	1.27	17.3
60	60	0.0657	1.27	19.33
70	72	0.0600	1.27	21.16

Table 2 indicates the characteristic oscillation depth,  $\delta$  is of the order of 1 millimeter (slightly less) for the frequency range observed, and the length ratio  $h/2\delta$  is much greater than unity. Table 3 gives an estimate of the pressure gradients ratio  $r_p$ . Here, in the absence of a precise measurement, both the oscillatory pressure gradient and the steady-flow pressure gradient have to be estimated. The maximum oscillatory pressure gradient is taken to be the ratio of the largest measured pressure amplitude to the quarter wave length. The steady pressure gradient can be computed from Eq. (7) for laminar flow. However, because of the uncertainty of the flow condition, estimates of the pressure gradient in turbulent (or transitional) flows are also given. Correspondingly, the pressure gradient ratios are listed for both the laminar and the turbulent flows. During the experiment, as the pressure oscillation increases in amplitude, the ratio of the pressure gradients also increases until the flame becomes anchored in the premixer. The listed pressure gradient ratios correspond to this final maximum value.

From Table 3, we see that the pressure gradient ratios are much greater than one. In other words, the experimental data are suggesting that the oscillating pressure gradient amplitude has to be much larger than the steady-flow pressure gradient to have flame-flashback. The analysis of the influence of  $r_p$  on flow reversal is therefore of interest.

Table 3. Estimated Pressure Gradients Ratio

$U_m$	$\omega$	quarter wave length $l/4$	max half oscill. amp. $\Delta p_{\max}$	max $\rho p' / \partial x$ ( $=\Delta p' / (l/4)$ )	$\partial \bar{p} / \partial x$ (laminar)	$\partial \bar{p} / \partial x$ (turbulent)	max $r_p$ (laminar)	max $r_p$ (turbulent)
ft/s	Hz	ft	psi	psi/ft	psi/ft	psi/ft		
40	48	9.5	0.4	0.0421	0.000364	0.0007 ~ 0.002	115	17 ~ 60
60	60	7.5	0.7	0.0933	0.000546	0.001 ~ 0.004	171	23 ~ 93

V.5. *Critical Pressure Gradients Ratio for Flow Reversal*

For  $h/2\delta \gg 1$ , the critical (minimum) pressure gradients ratio needed for flow reversal can be found by looking at the limit  $2y/h \ll 1$ . This is because flow reversal always first occurs near the wall. In this limit, Eq. (8) reduces to

$$u'/(a/\omega) = (\cos\omega t + \sin\omega t) \frac{y}{\delta} \quad (12)$$

This shows that the oscillatory velocity component near the wall first increases from  $\omega t = 0$  to  $45^\circ$  and then decreases from  $45^\circ$  to  $225^\circ$ . Since the oscillatory pressure gradient is proportional to  $\cos\omega t$ , the near wall velocity response lags behind the pressure gradient by  $45^\circ$ . Since the minimum  $u'$  occurs at  $\omega t = 225^\circ$ , this is the angle for determining the flow reversal limit. Using Eqs. (6), (10) and (12), it can be shown that the critical pressure gradient ratio is given by

$$[r_p]_{cr} = \sqrt{2} \left[ \frac{h}{2\delta} \right] \quad \text{for} \quad \frac{h}{2\delta} \gg 1 \quad (13)$$

In the limit  $h/2\delta \ll 1$ , Eq. (8) reduces to

$$\frac{u'}{u} = \frac{3}{2} r_p \cos\omega t \left[ 2 \left[ \frac{2y}{h} \right] - \left[ \frac{2y}{h} \right]^2 \right] \quad (14)$$

The above equation shows that in the diffusive-thin limit ( $h/2\delta \ll 1$ ), the oscillatory velocity is in phase with the pressure gradient. Using Eqs. (6) and (14), the critical pressure gradient ratio is found to be one.

Figure 22 gives the computed  $(r_p)$  as a function of  $h/2\delta$ . It can be seen that for  $h/2\delta > 3$ , Eq. (13) applies, and for  $h/2\delta < 0.3$ ,  $(r_p)_{cr} \approx 1$ . Referring to Table 2, for the experiment at  $u_m = 40 \text{ ft/sec}$ ,  $h/2\delta$  is equal to 17.3, from Eq. (13) or Fig. 22,  $(r_p)_{cr} = 24.47$ ; and for  $u_m = 60 \text{ ft/sec}$ ,  $(r_p)_{cr} = 26.87$ . Both values fall into the range of  $r_p$  estimated in Table 3. However, for a substantial extent of flow reversal (higher reverse velocity and greater flow reverse duration within one cycle), pressure gradient ratio greater than  $(r_p)_{cr}$  is needed. This will be shown in the next section using the velocity profiles corresponding to several values of  $R_p$ .

#### V.6. *Velocity Profiles Near the Wall*

Fig. 23 presents the near-wall velocity profiles as a function of  $\omega t$  (in degree) for  $r_p = 50$  and  $h/2\delta = 17.3$  (this value corresponds to  $\omega = 48 \text{ cps}$ ). The profiles show that very close to the wall, the velocity decelerates from  $45^\circ$  to  $225^\circ$  as indicated by Eq. (12). Moderate flow reversal occurs both in terms of magnitude, penetration depth and duration of reversal. This figure also shows that there is a time lag between the near-wall velocity profiles and those further into the channel interior. For example, comparing the profiles at  $225^\circ$  and  $270^\circ$ , near the wall, flow is accelerated from  $225^\circ$  to  $270^\circ$ , but away from the wall, the flow is still decelerated during the same period. This time lag mechanism also produces the wavy profile indicated by the curve at  $315^\circ$ .

At  $r_p = 100$ , Fig. 24 shows the extent of flow reversal is greatly increased resulting in a higher reversed velocity and greater depth of flow reversal layer. Furthermore, an interesting phenomenon is shown by the velocity profile at  $315^\circ$ , i.e. a flow reverse region exists in the fluid interior ( $0.9 < y/\delta < 2.0$ ), while the flow near the wall is not reversed.

The velocity profiles for a  $r_p$  close to the critical value  $\left[ \left[ r_p \right]_{cr} = 24.47 \right]$  are shown in Fig. 25. For  $r_p = 30$  at  $h/2\delta = 17.3$ , flow reverses near the wall but its extent is very small.

Since we are studying flame flashback in the premixing channel, factors contributing to greater flashback potential are of interest. Obviously, higher reverse velocity and greater flow reverse duration (within one cycle) would favor a greater upstream distance for the flame to travel. Another factor which should be considered is the depth of flow reversal from the wall. This is relevant because flame may quench near the wall. Fig. 26 presents the maximum reversal velocity  $\left[ u_{rev}/\bar{u} \right]$ , the maximum flow reversal depth  $\left[ y_{rev}/\delta \right]$  and the duration of flow reversal within one cycle  $\left[ \Delta\theta_{rev}$ , in degrees  $\right]$  as a function of the ratio of pressure gradients  $r_p$  for  $h/2\delta = 17.3$ . It can be seen that all of the three curves increase monotonically with  $r_p$ .

Before we discuss the effect of  $r_p$  on flame flashback, we would like to say a few words about the velocities far from the wall.

The velocity at the centerline of the channel can also be obtained for  $h/2\delta \gg 1$  by taking the limit  $2y/h \rightarrow 1$ . In this limit, Eqs. (8) and (9) reduce to:

$$\left(\frac{u'}{u}\right)_{\frac{2y}{h}=1} = \frac{3}{2} \left(\frac{2\delta}{h}\right)^2 r_p \sin\omega t$$

The above equation shows that the centerline velocity lags 90 degrees behind the pressure gradient and has a 45 degrees lag behind the velocity response near the wall. Furthermore, the pressure gradient ratio for a centerline flow reversal is found to be proportional to the square of  $h/2\delta$ . In contrast, Eq. (13) shows that the critical  $r_p$  for wall velocity reversal is proportional to the first power of  $h/2\delta$ . In the limit of large  $h/2\delta$ , therefore, the oscillatory pressure gradient amplitude has to be much larger to cause the flow to reverse at the centerline.

#### V. 7. *Flame Flashback in Oscillatory Flow*

How does flow oscillation (in particular, velocity reverse) affect the flame flashback characteristics? To answer this question in a quantitatively correct manner, we feel a basic aerothermomechanical analysis including multi-dimensional effect and unsteady term is needed. For steady state such a model has been used in Ref. 8 for a laminar system. What has to be extended from that analysis is the inclusion of unsteadiness and possibly turbulence.

In the absence of such an elaborate model, can we use the classical phenomenological approach of Lewis and von Elbe (1961)

to predict qualitative trend? In the following, such an attempt will be made.

Lewis and von Elbe's approach is based on velocity comparison at the edge of the wall quenching layer. If the flame burning velocity is greater than the mixture opposed flow velocity, flashback will occur. In principle, this idea can be applied to oscillatory flows if the instantaneous flow velocity profile is specified. The other two quantities needed in this approach is the quenching distance and the mixture burning velocity.

The data on quenching distance and laminar burning velocity for lean propane-air flames at 800 K have been hard to find. Based on the expression given by Andrew and Bradley (1972) for methane-air systems, we estimate the laminar burning velocity to be  $4 \pm 1$  ft/s and the quenching distance to be around 1 mm for propane-air equivalence ratio of 0.6. The precision of these numbers is perhaps poor, but it is not too essential for the following qualitative argument.

Using Table 2, the quenching distance 1 mm is located at  $y/\delta = 1.36$ . At that height, for pressure gradient  $r_p = 30$ , Fig. 25 shows that the velocity profile at  $270^\circ$  gives  $u/u_m = 0.09$  which corresponds to  $u = 3.6$  ft/sec. For a burning velocity of 4 ft/s, the flame can propagate into the premixer. However, since the net upstream velocity is small and the duration of a positive upstream propagation is short, only tiny flickering should be observed. For a higher  $r_p = 50$ , Fig. 26 shows that at the edge of the quench layer

( $y/\delta = 1.36$ ), the flow velocity is actually reversed, so greater velocity into the premixer is produced. This, plus the longer flow reversal duration, should result in a longer distance for the flame to flashback into the premixing channel. This trend is greatly accelerated as the pressure gradients ratio is further increased as shown by Figs. 24 and 26.

The above qualitative description seems consistent with what has been observed experimentally. Quantitative prediction is more difficult, however. Take quenching distance, for example. Normally, it is determined by passing a flame into a narrow channel or a small diameter tube in a quiescent mixture. In the case when there is a transient reversal, the wall layer may consist of hot combustion products drawn from the dump plane. The meaning of quenching distance is less clear in this situation. Furthermore, the hot wall of the experiment makes definition of a quench layer even more ambiguous.

The second uncertainty has to do with turbulent flow which will be briefly mentioned in the next section.

#### V.8. *Status of Modeling Periodic Turbulent Flow in Pipes*

As mentioned earlier in Section V.2, the flow in the premixing channel may well be turbulent. That being the case, one may think that the laminar flow analysis just presented is irrelevant because the turbulent flow is known to have much steeper velocity gradient near the wall. We think, however, the laminar flow analysis does yield the correct trend and the quantitative predictions on critical pressure

gradient ratio, reverse depth and duration of flow reversal may not be as bad as one might first think, for the following reason.

The steeper turbulent wall velocity profile is the result of the much larger effective kinematic viscosity, but this same larger kinematic viscosity is also helping the oscillation to reverse the flow more effectively by increasing the oscillation depth  $\delta$  (see Eq. (9)).

Needless to say, a turbulent flow analysis is justified. The status of modeling work on turbulent oscillating flow in pipes can be summarized by using the work of Acharya and Reynolds (1975) and Tu and Ramaprian (1983). Both works employ a one-equation ( $k$ , turbulent kinetic energy) turbulence model with turbulent scale prescribed as a function of radial distance. This model has been used very successfully for steady flows but it failed for periodic flow at high frequencies. We expect it will be even more likely to fail in our case because of the larger oscillatory pressure gradient. The reason for failure is probably that the turbulent length scale is assumed to be time-independent. A logical next step seems to be the relaxation of this assumption by using the  $k$ - $\epsilon$  model.

## CHAPTER VI

### CONCLUSIONS AND RECOMMENDATIONS

In this study, visual access to the combustion process proved most useful. Not only were several stages of burning identified as in section 4.1, but also the upstream propagation of the flame with the leading edge near the wall was verified with high speed photography. The oscillatory nature of the flame was recorded on film and determined to be of the same frequency as that recorded with pressure transducers.

The parametric study of the effects of inlet and premixer wall temperature and premixer velocity on the equivalence ratio created a data base from which a few conclusions are drawn. First, the effect of inlet air temperature is slight. However, it is evident that the flashback equivalence ratio decreases as the inlet air temperature increases. Second, the premixer wall temperature and premixer velocity are not governing variables over flashback. Third, the parametric study using the average premixer velocity does not support the steady-state velocity balance concept as the flashback mechanism.

It appears that combustion instabilities (spontaneous pressure oscillations) play an important role in the occurrence of flashback. In the test conducted, the amplitude of pressure oscillations were

always observed to increase with the flickering penetration distance and reach a maximum amplitude just prior to maintained flashback. The estimated oscillatory pressure gradient is many times greater than the mean pressure gradient in the premixer. A theoretical analysis shows that, in such a condition, the flow will reverse in the premixer boundary layer. A simple test using ceramic tufts verified that flow reversals did occur at the premixer exit during flickering. This leads one to conclude that flashback occurs as the result of a local flow reversal caused by combustion instability.

With these thoughts in mind several recommendations can be made to further the understanding of flashback. First, an efficient experimental technique should be developed to determine the velocity profile in the premixing tube near the wall both before and during flashback. The intent would be to determine the location, magnitude and duration of flow reversals. Second, pressure gradients for both the oscillatory and non-oscillatory states should be measured. Third, the criterion for recording data should be such that randomness is reduced. Instead of recording conditions for flame stabilization at the 1/4 in. step, which was a marginal stabilizer, data should be taken when the flame extended a certain distance into the premixer. The randomness of the data may also be reduced by plotting different parameters such as pressure oscillation amplitude and frequency. Fourth, the analysis of flow reversal should be extended to turbulent flow. Last, but not least, an understanding of the mechanism of combustion instability is needed. Since combus-

tion oscillation and flame flashback are coupled in prevaporized-premixed combustors, prevention of flashback will be difficult without the elimination or the control of combustion instability.

Premixed combustor development should include observation, high-speed cine records, and high frequency pressure records to identify conditions or geometries which tend to cause unstable burning likely to lead to flashback.

## REFERENCES

1. Acharya, M. and Reynolds, W.C., 1975, "Measurements and Predictions of a Fully Developed Turbulent Channel Flow with Imposed Controlled Oscillations," Tech. Report No. TF-8, Dept. Mech. Engr., Stanford University.
2. Andrew, G.E., and Bradley, D., 1972, "Burning Velocity of Methane-Air Mixture," Combustion and Flame, 19:275-288.
3. Anonymous, 1980. "Procedure for the Continuous Sampling and Measurement of Gaseous Emissions from Aircraft Turbine Engines." SAE ARP 1256A.
4. Coats, C.M., 1980. Comment on "Review of Flashback Reported in Prevaporizing/premixing Combustion." Combustion and Flame, 37:331-338.
5. Ganji, A.R., and Sawyer, R.F., 1980. Blowout and Flashback in a Two Dimensional Lean Premixed Combustor. Department of Mechanical Engineering, University of California. NASA Grant NSG-3028.
6. Keller, J.O., et. al, 1981. Mechanism of Instabilities in Turbulent Combustion Leading to Flashback. AIAA Journal, Vol. 20, No. 2.
7. Landau, L.D. and Lifshitz, E.M., 1959. Fluid Mechanics, Pergamon Press, p. 95.
8. Lee, S.T., and T'ien, J.S., 1982. A Numerical Analysis of Flame Flashback in a Premixed Laminar System. Combustion and Flame 48:273-285.
9. Lewis, B., and von Elbe, G., 1961. Combustion, Flames and Explosions of Gases, pp. 220-224, New York, Academic Press, Inc.
10. Plee, S.L., and Mellor, A.M., 1978. Review of Flashback Reported in Prevaporizing/Premixing Combustors. Combustion and Flame, 32:193-203.

11. Plee, S.L., and Mellor, A.M., 1980. Reply to Comments by C.M. Coats on "Review of Flashback Reported in Prevaporizing/Premixing Combustors." Combustors and Flame, 37:335-336.
12. Proctor, M.P., 1984. "Combustor Flame Flashback." M.S. Thesis, Dept. Mech. & Aero. Engr., Case Western Reserve University.
13. Propulsion Chemistry Division, Barnett, H.C. and Hibbard, R.R. editors, 1959. "Basic Considerations in the Combustion of Hydrocarbon Fuels with Air." NACA Report 1300.
14. Putnam, A.A., and Jensen, R.A., 1949. Application of Dimensionless Numbers to Flash-Back and Other Combustion Phenomena. Third Symposium on Combustion, Flame and Explosion Phenomena, pp. 89-98. Baltimore, Maryland, The Williams and Wilkins Company.
15. Reshotko, E., 1984. Private communication.
16. Tu, S.W. and Ramaprian, B.R., 1983. "Quasi-steady Modeling of Periodic Turbulent Pipe Flows." IHR-TC-1, Iowa Institute of Hydraulic Research, The University of Iowa.

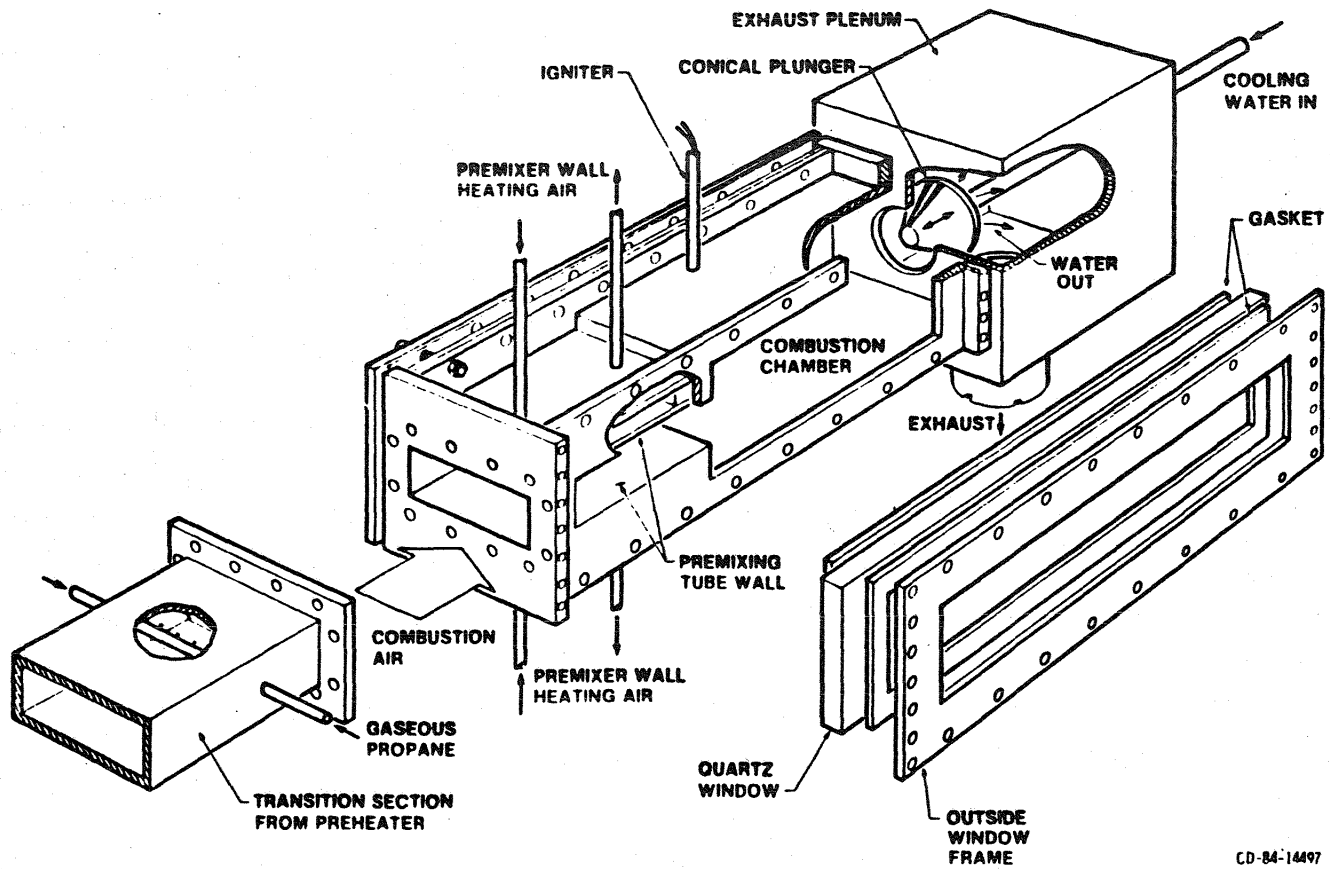


Figure 1a. Combustor test section.

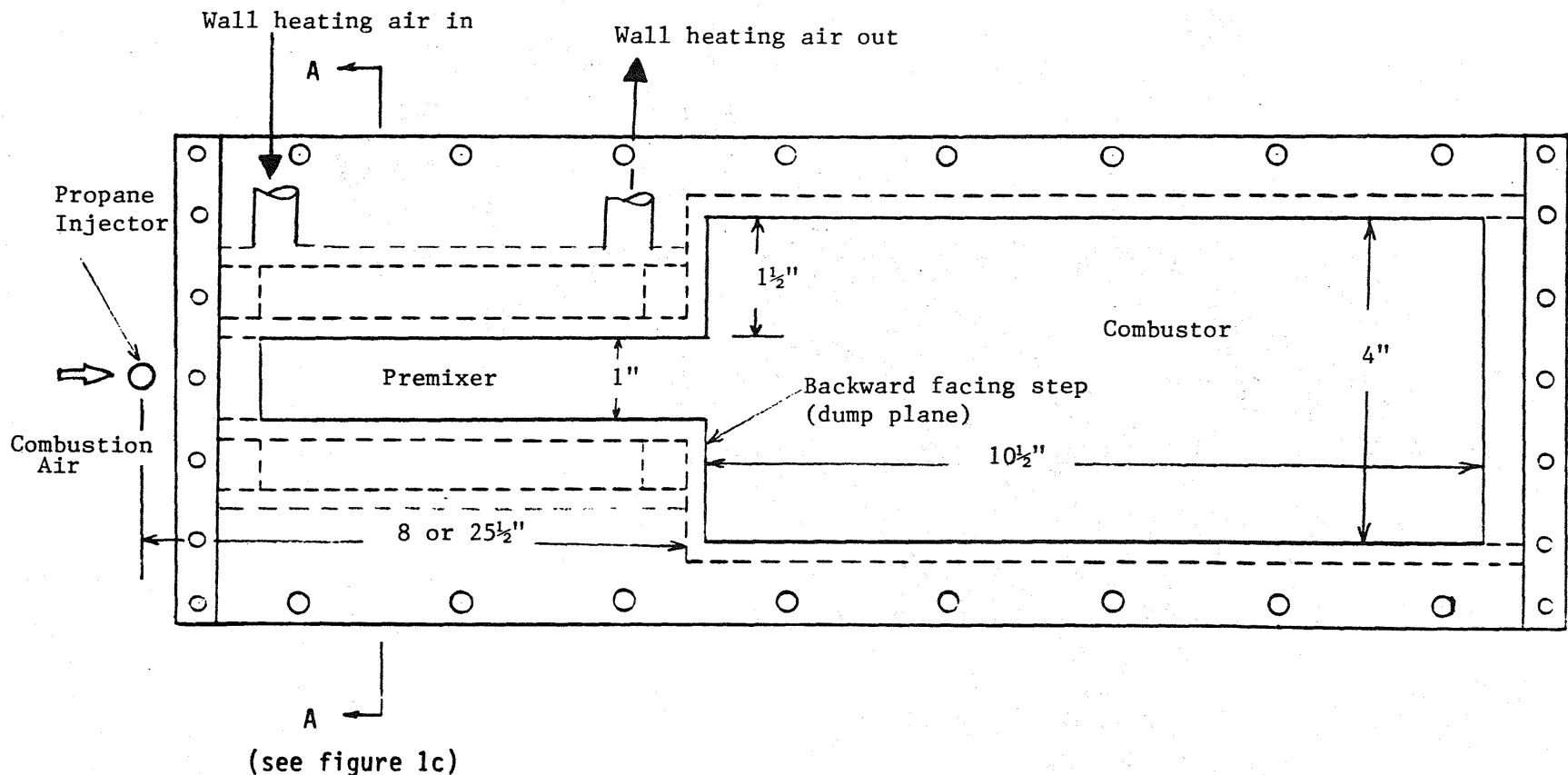
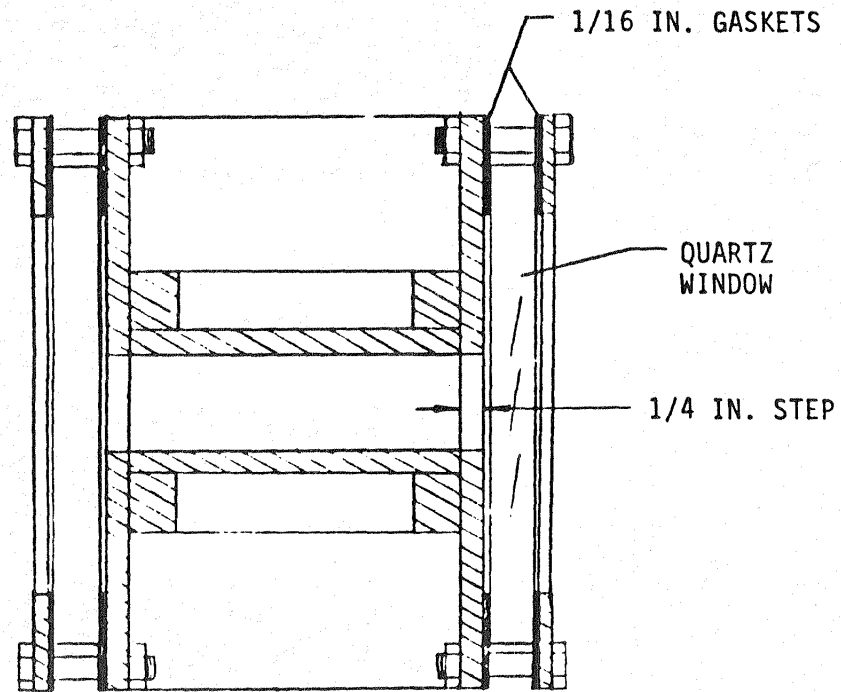


Figure 1b. Sideview of combustor test section.



SECTION A-A

Figure 1c. Section view of test section. (looking downstream)  
See figure 1b.

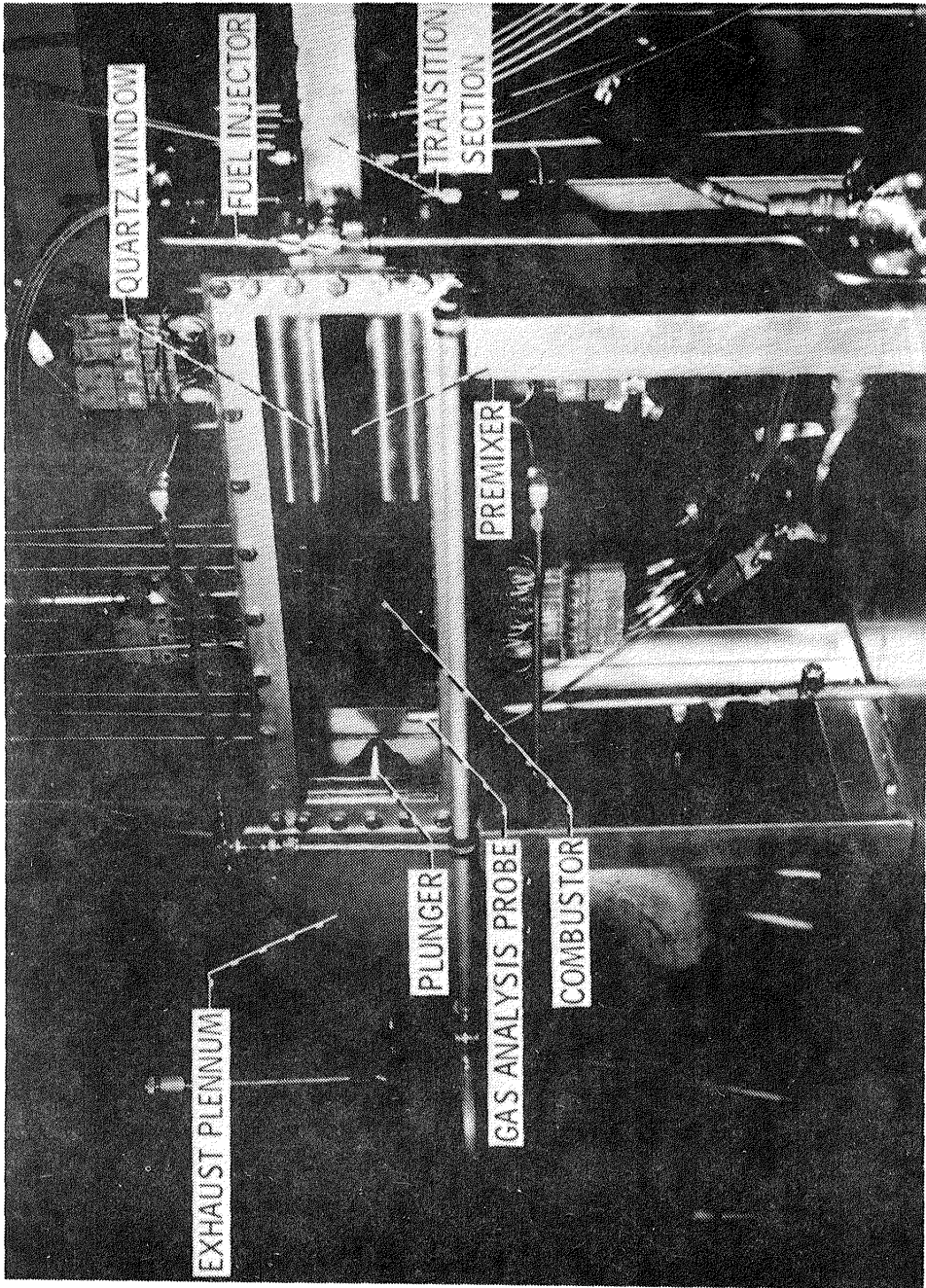


Figure 2. Photograph of combustor test section.

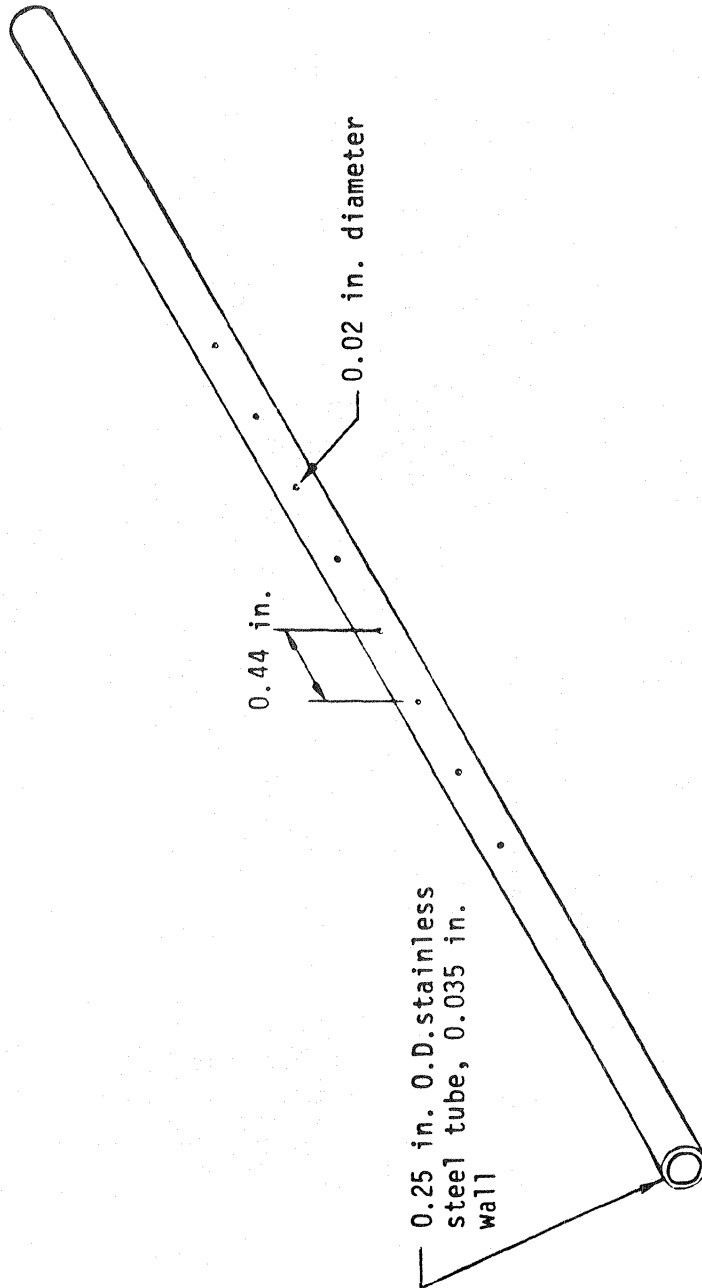


Figure 3. Fuel injector.

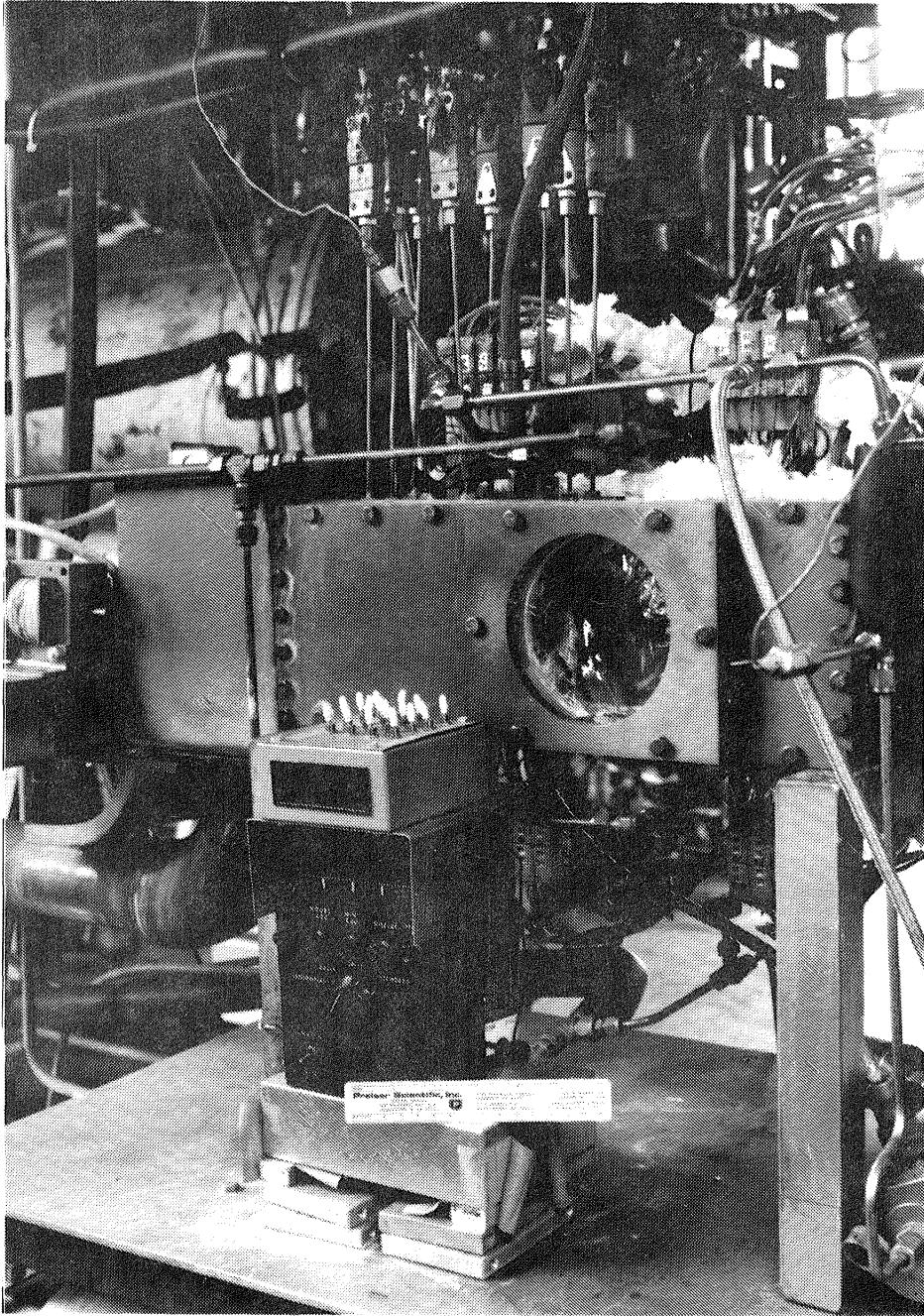


Figure 4. Test section with 6in. round window.

- WALL THERMOCOUPLES
- STREAM THERMOCOUPLES
- PRESSURE TRANSDUCER AND STREAM THERMOCOUPLE
- ⊠ IGNITER

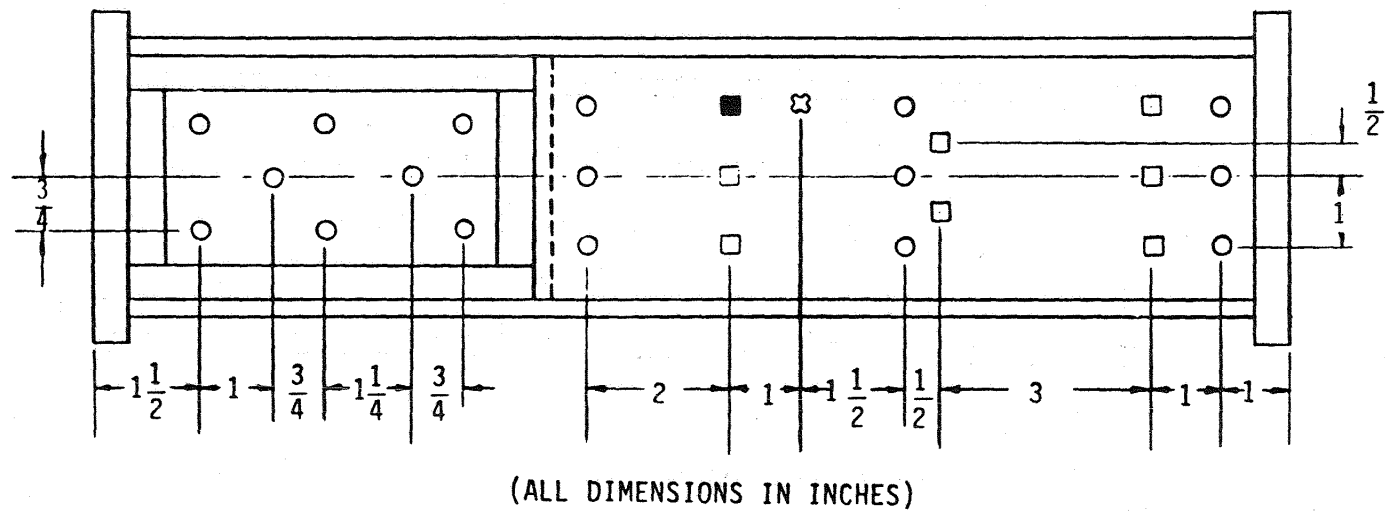
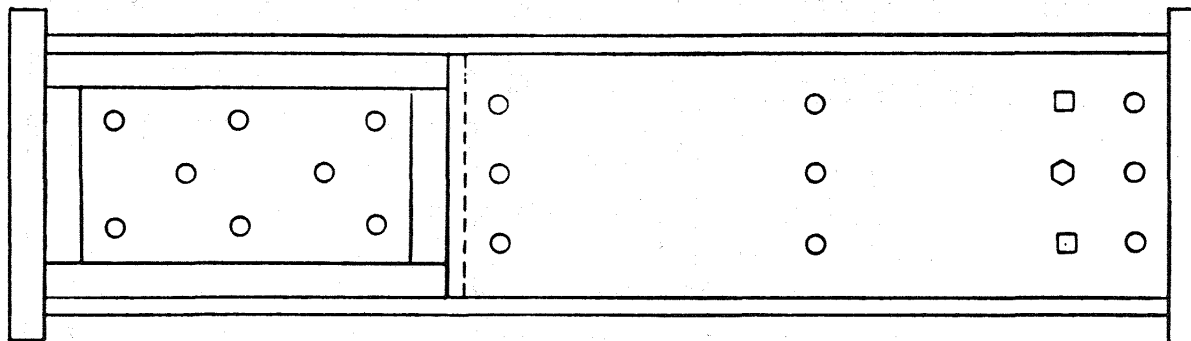


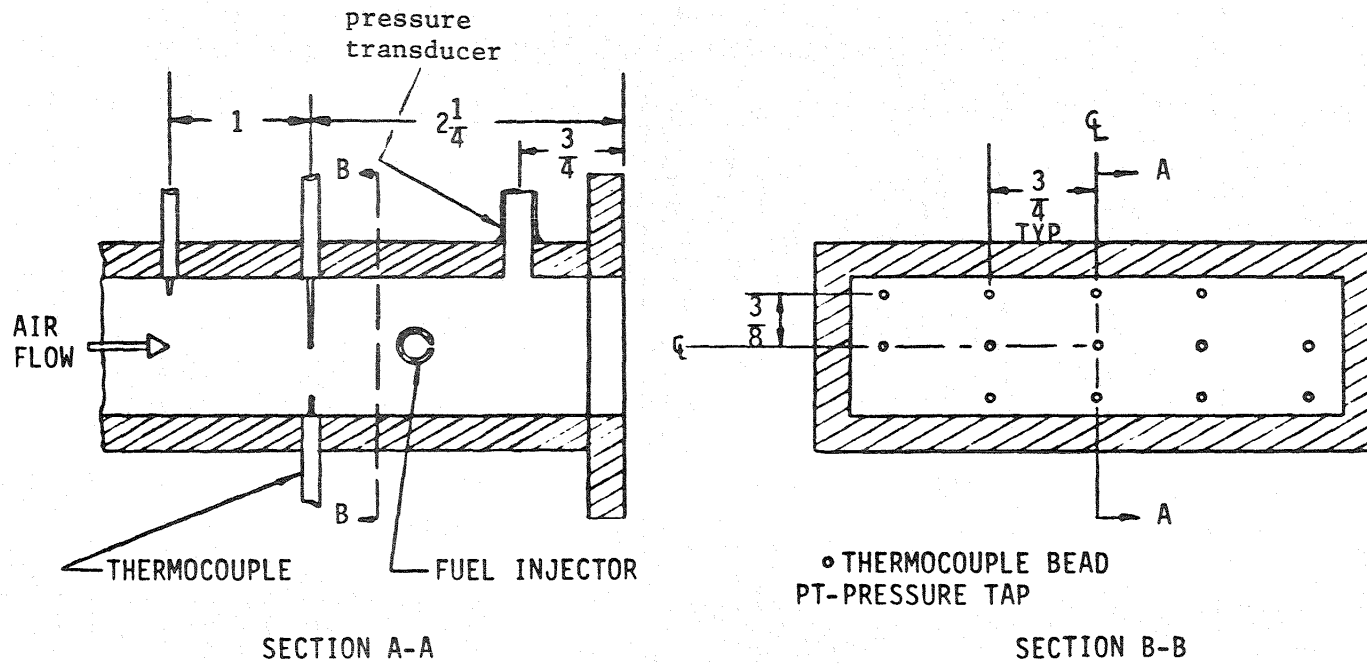
Figure 5. Thermocouple, pressure transducer, and igniter locations in top wall.

- WALL THERMOCOUPLES
- STREAM THERMOCOUPLES
- ◊ GAS ANALYSIS PROBE



(DIMENSIONS SAME AS FIGURE 5.)

Figure 6. Thermocouple and gas analyzer locations in bottom wall.



(ALL DIMENSIONS IN INCHES)

Figure 7. Inlet thermocouple and pressure tap locations in transition section.

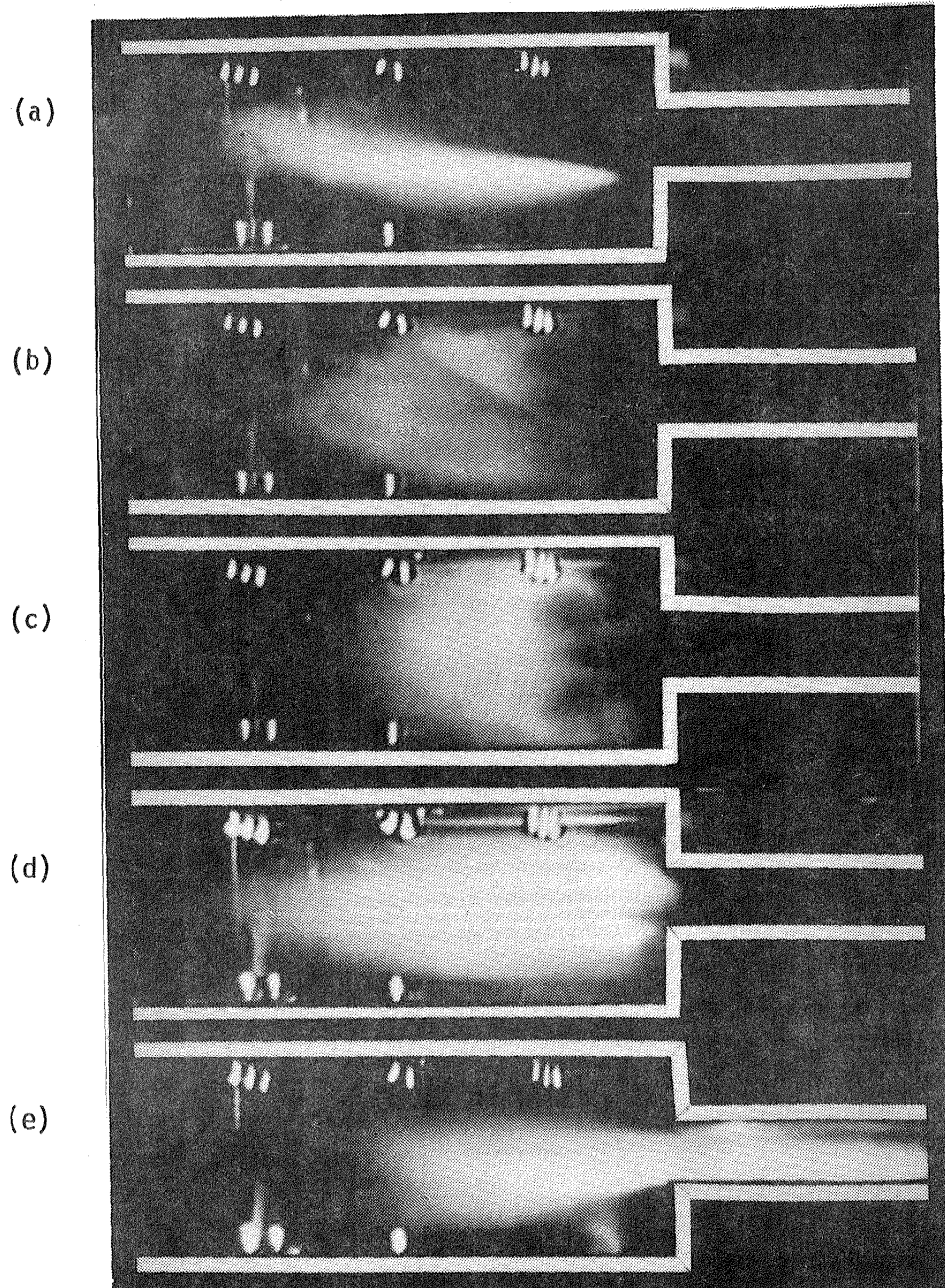


Figure 8. Different stages of burning. (a) and (b), lean flames, equivalence ratio, 0.41; (c) recirculation zones formed behind step, equivalence ratio, 0.44; (d) flame began flickering, equivalence ratio, 0.56; (e) maintained flashback, equivalence ratio, 0.60. Inlet air temperature, 850K; premixer wall temperature, 750K; average premixer velocity, 70 ft/s; fuel injector 8 in. upstream of step.

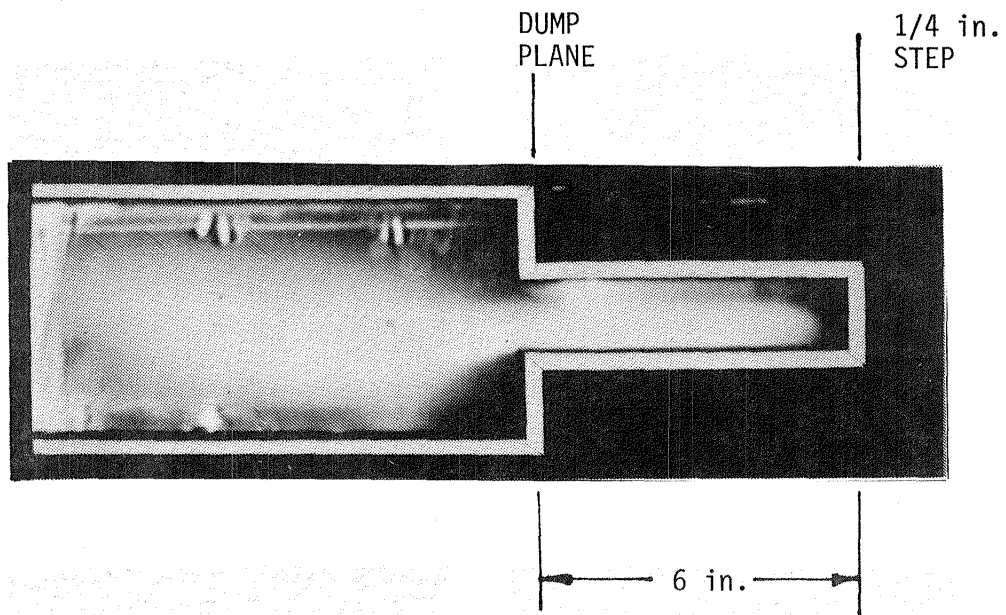


Figure 9. Flame stabilized at 0.25 in. step in premixer. Inlet air temperature, 850K; premixer wall temperature, 800K; average premixer velocity, 111 ft/s; equivalence ratio, 0.56.

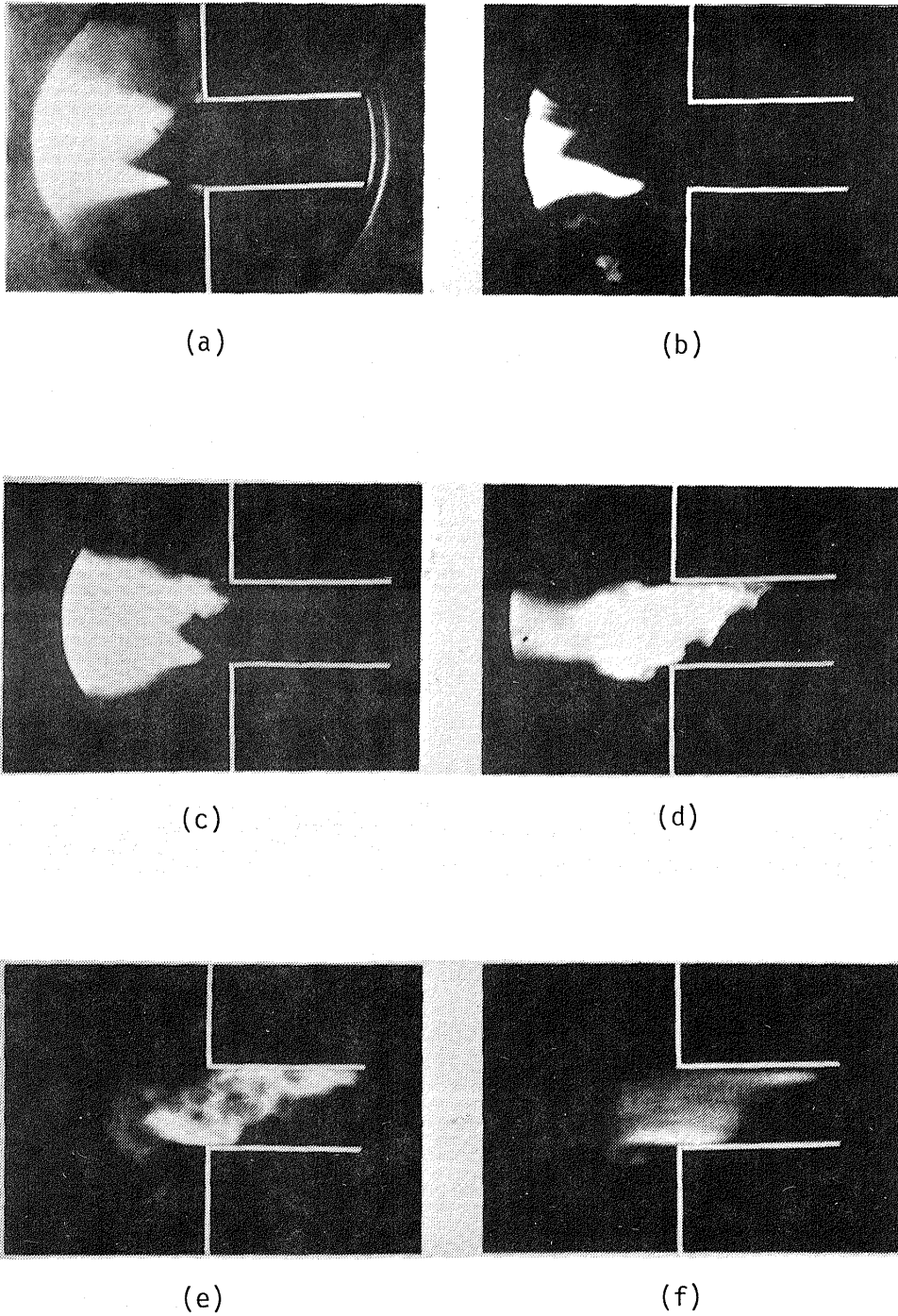


Figure 10. Photographic sequence of flashback filmed through 6in. round window at dump plane. Flow is from right to left; time interval, 2.5 ms.

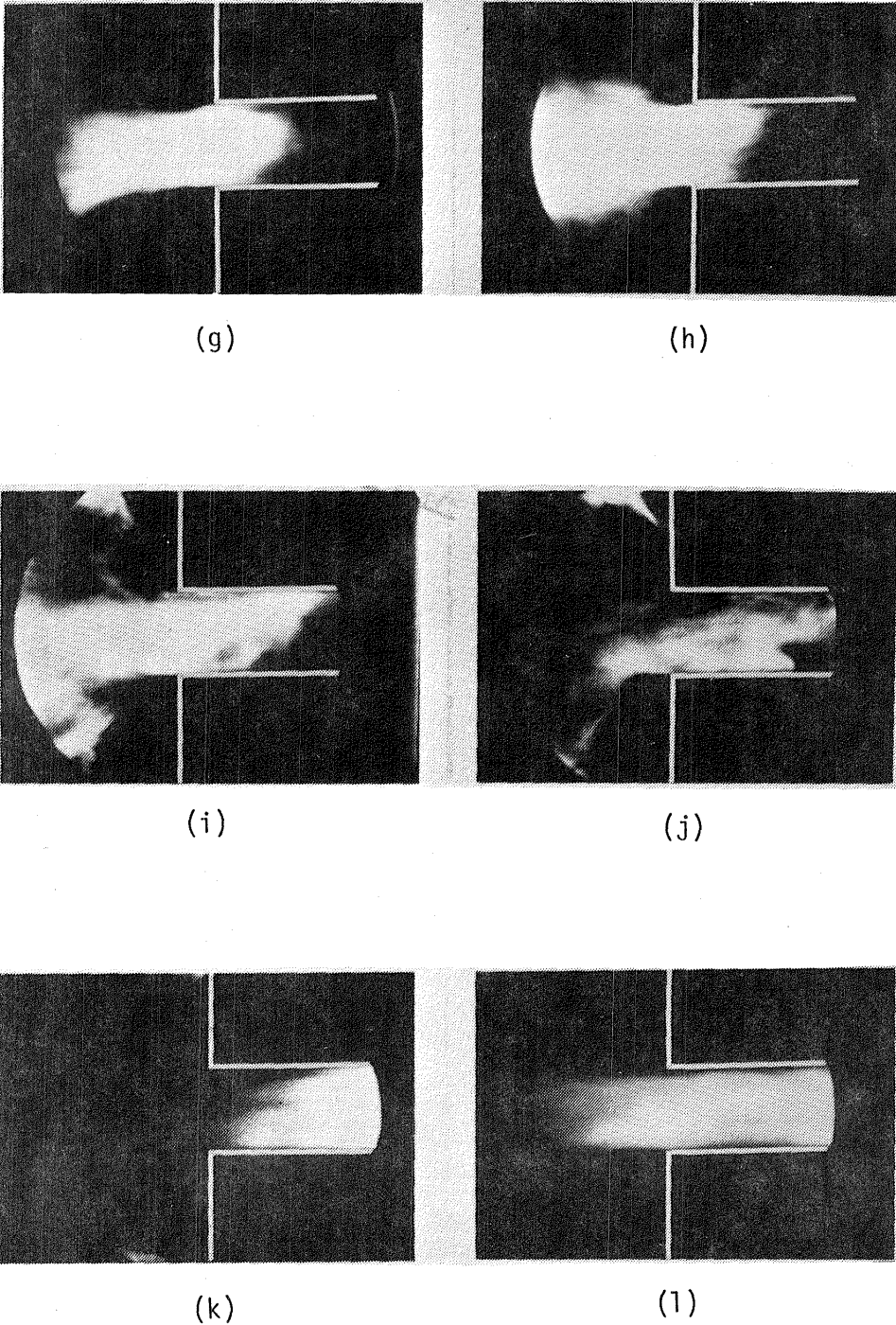


Figure 10. Concluded. Inlet air temperature, 830 K; pre-mixer wall temperature, 750 K; initial pre-mixer velocity, 86 ft/s. Maintained flashback induced at pre-mixer velocity, 76 ft/s; equivalence ratio, 0.48.

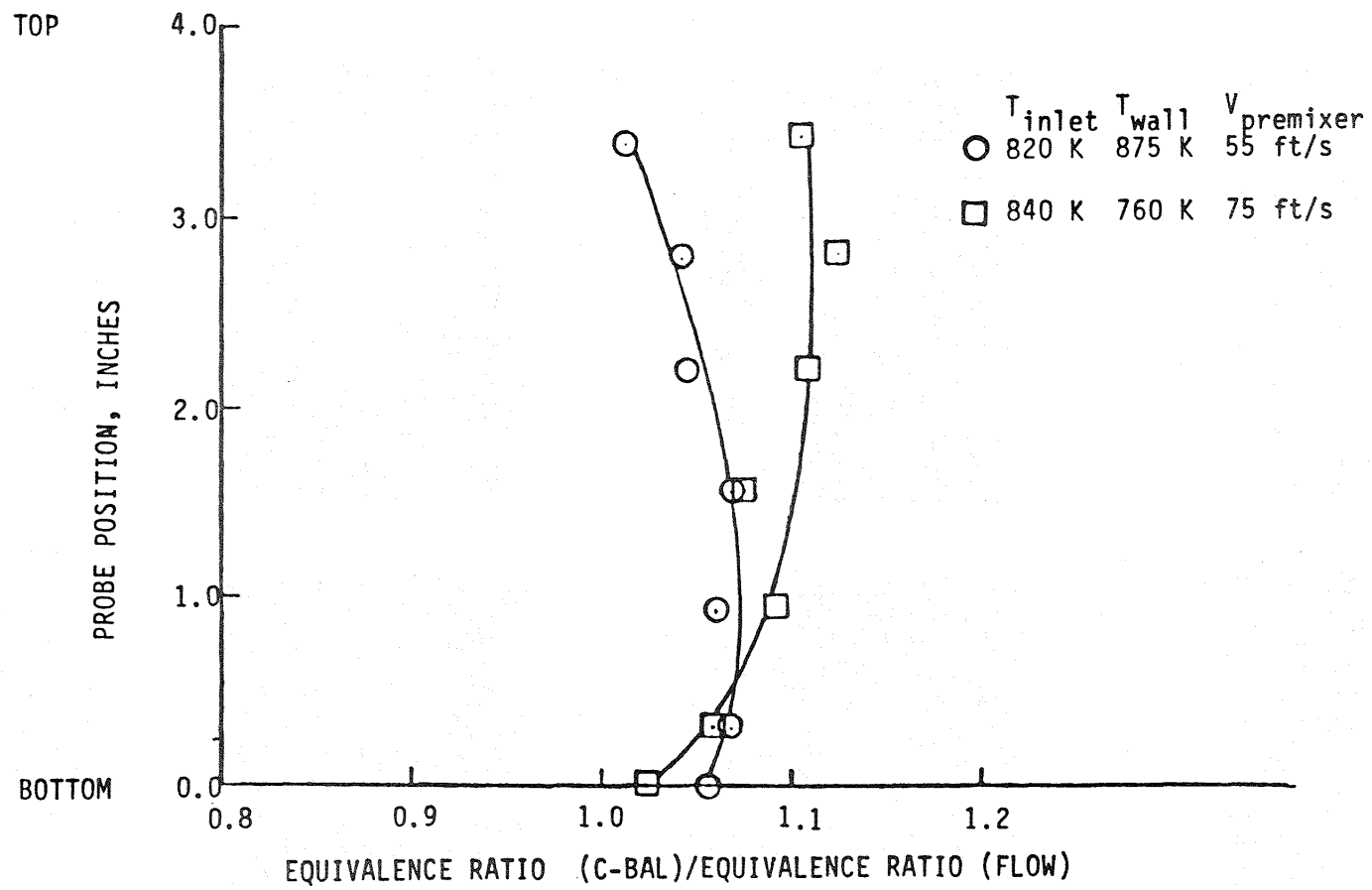


Figure 11. Gas emissions profile; equivalence ratio, 0.36-0.38.



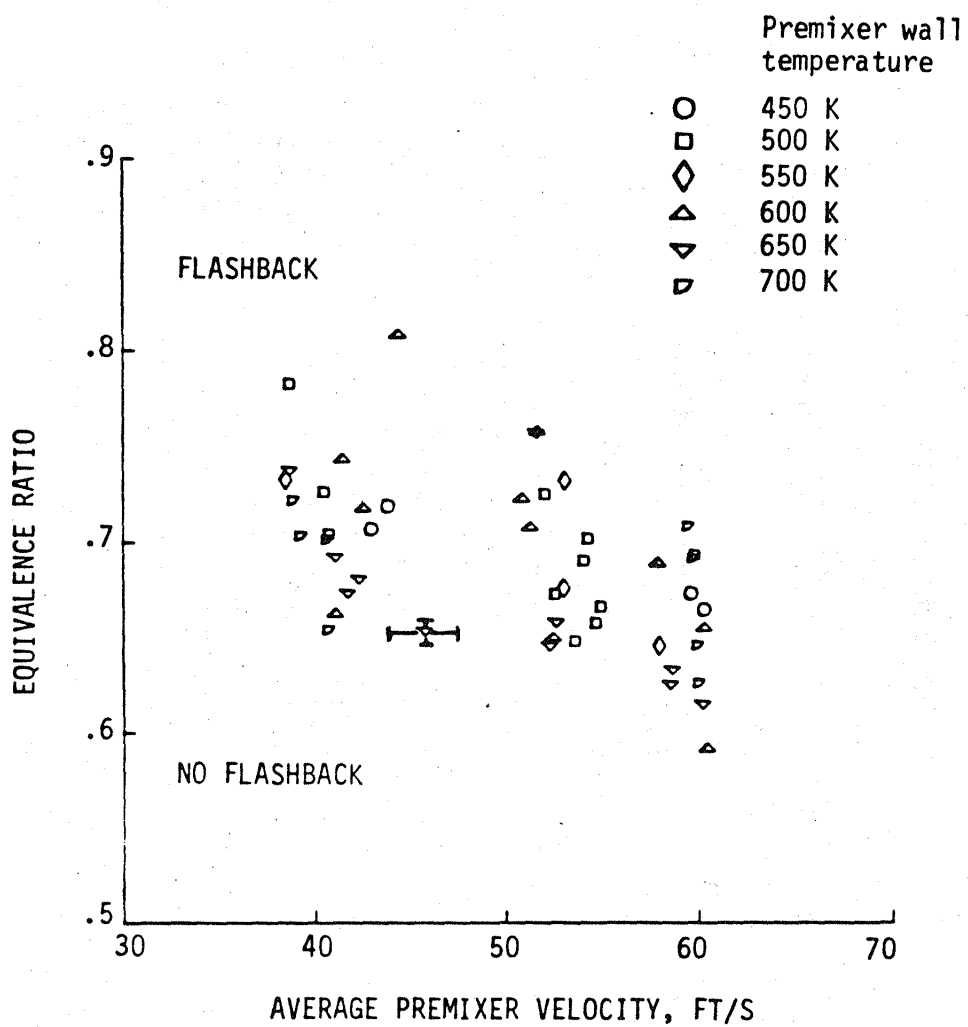


Figure 13. Effect of average premixer velocity and wall temperature on maintained flashback boundary. Inlet air temperature, 600K; fuel injector 8in. upstream of step.

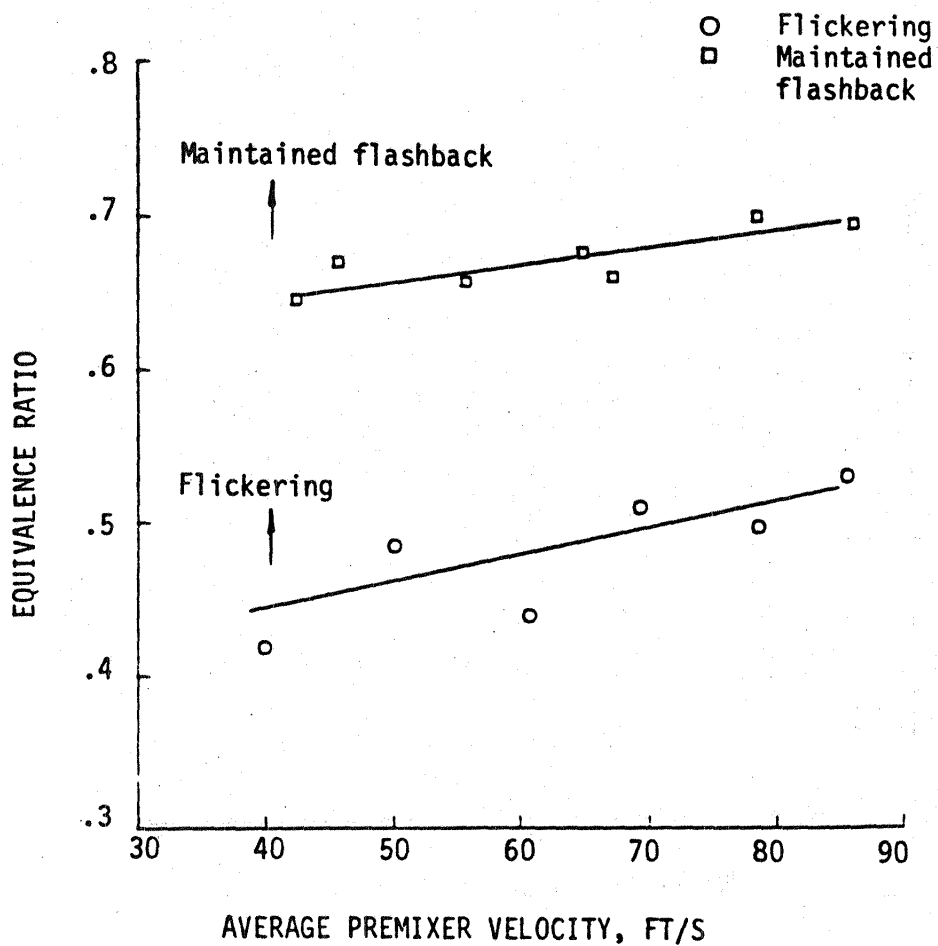


Figure 14. The difference between flickering and maintained flashback. Fuel injector  $25\frac{1}{2}$  in. upstream of step; inlet air temperature, 750K; premixer wall temperature, 700K.

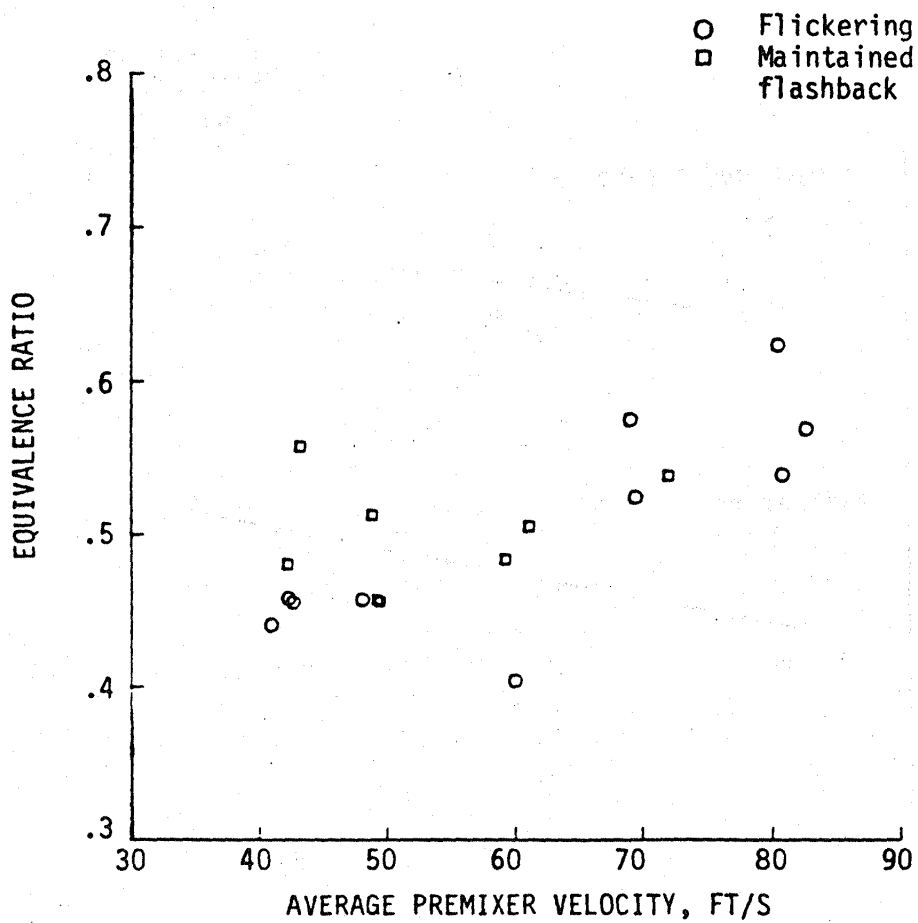


Figure 15. The difference between flickering and maintained flashback. Fuel injector 25½ in. upstream of step; inlet air temperature, 700K; premixer wall temperature, 700K.

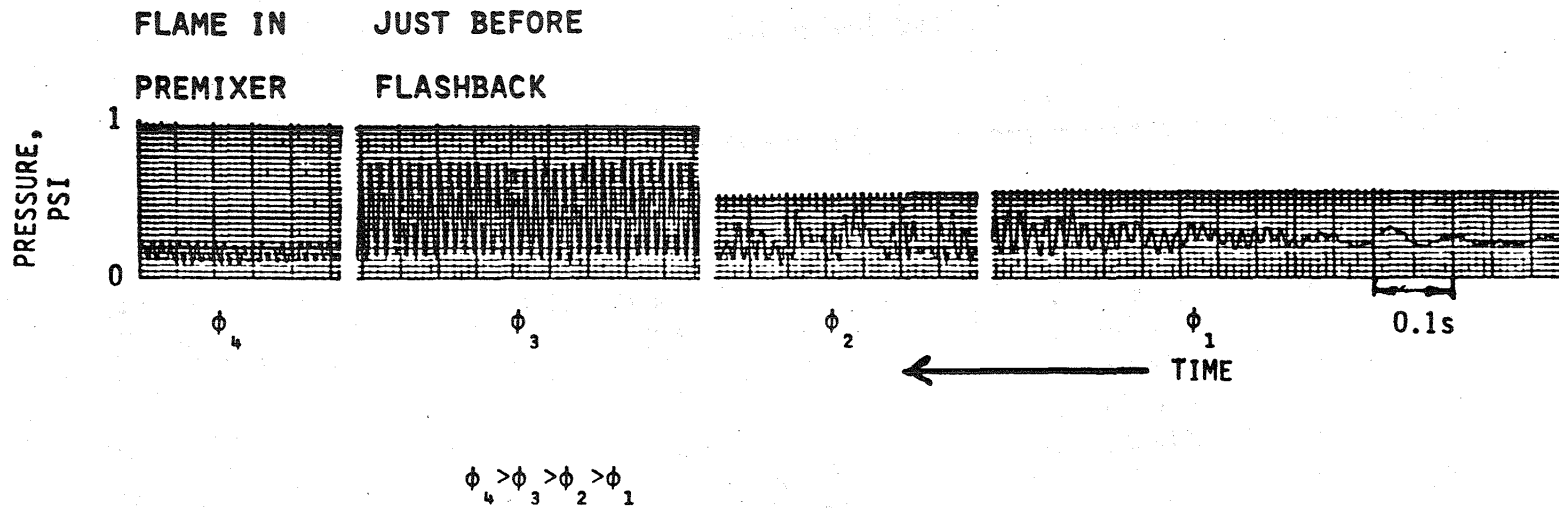


Figure 16. Typical effect of equivalence ratio on combustor pressure oscillations.

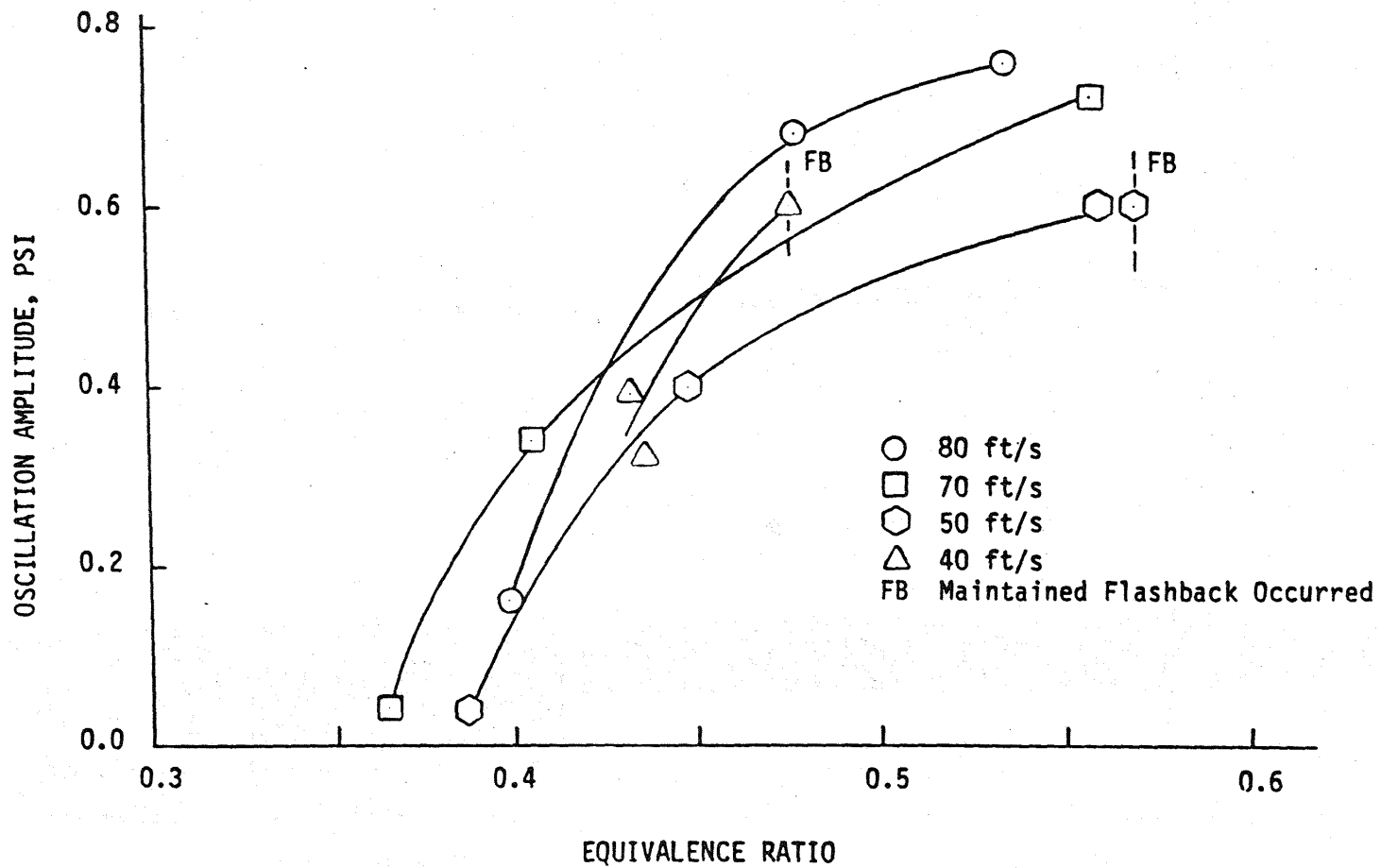


Figure 17. Effect of equivalence ratio on pressure oscillation amplitude at several premixer velocities. Inlet air temperature, 650 K; premixer wall temperature, 750 K; fuel injector 8 in. upstream of the step.

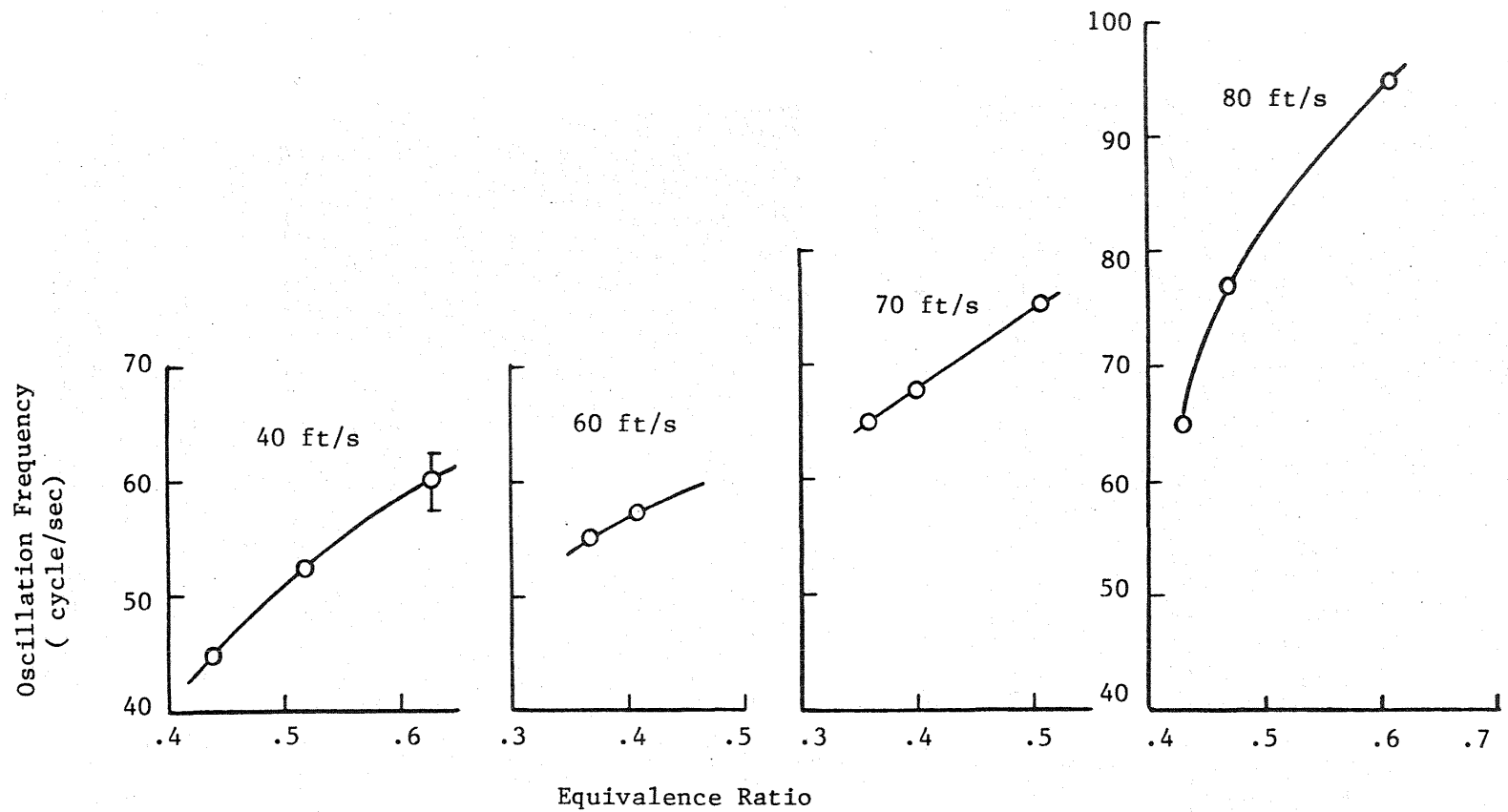
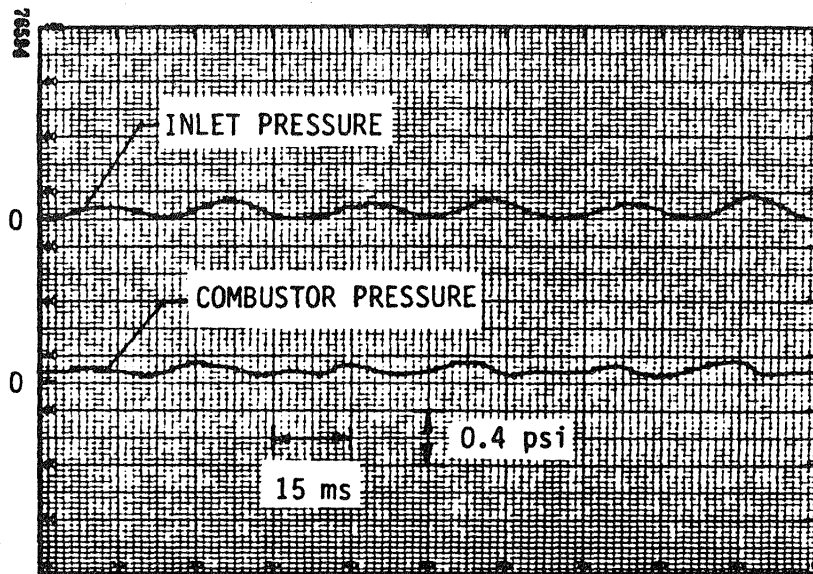
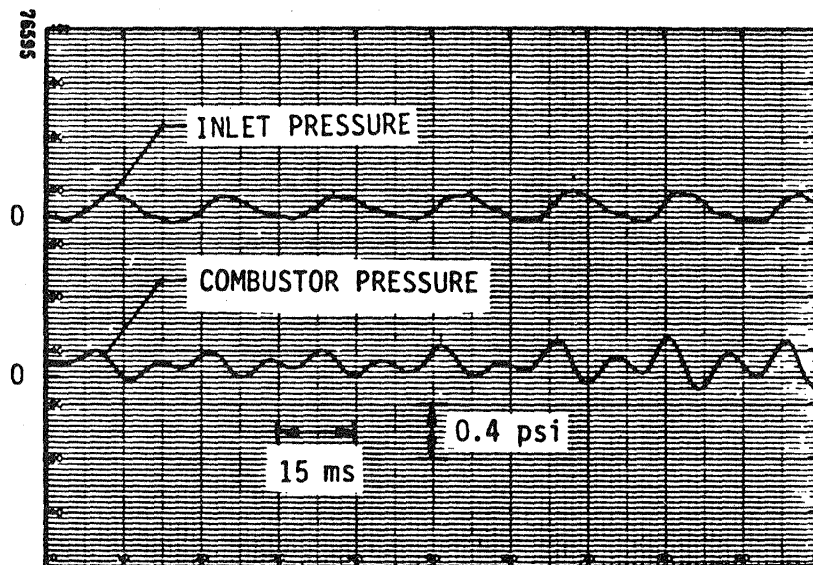


Fig. 18. Effect of premixer velocity and equivalence ratio on combustor pressure oscillation frequency while flame on step. Inlet air temperature, 650K; premixer wall temperature, 750K.

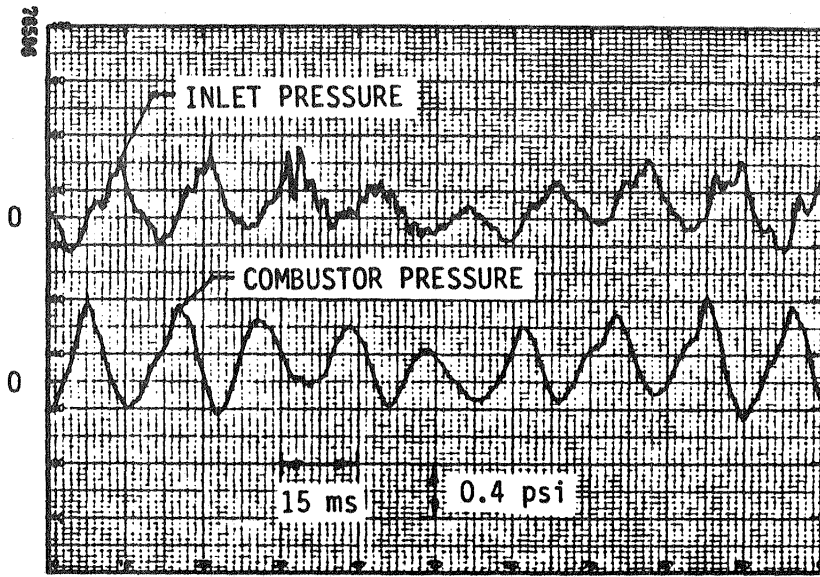


(a) Equivalence ratio, 0.398; flame on step.  
(behind dump plane)

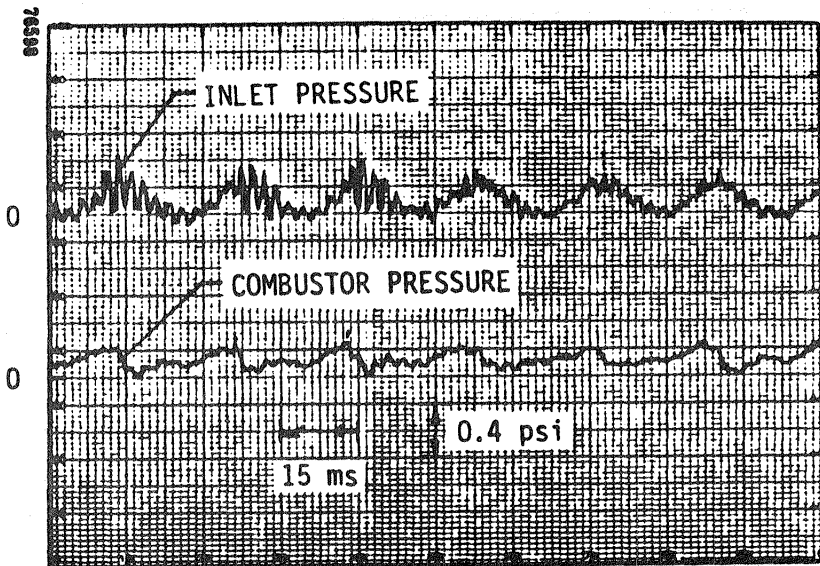


(b) Equivalence ratio, 0.426; flame flickering.

Figure 19. Inlet and combustor pressure traces at inlet air temperature, 700K; premixer wall temperature, 720K; average premixer velocity, 45 ft/s; fuel injector 8in. upstream of step; pressure taps 43.75in. apart.

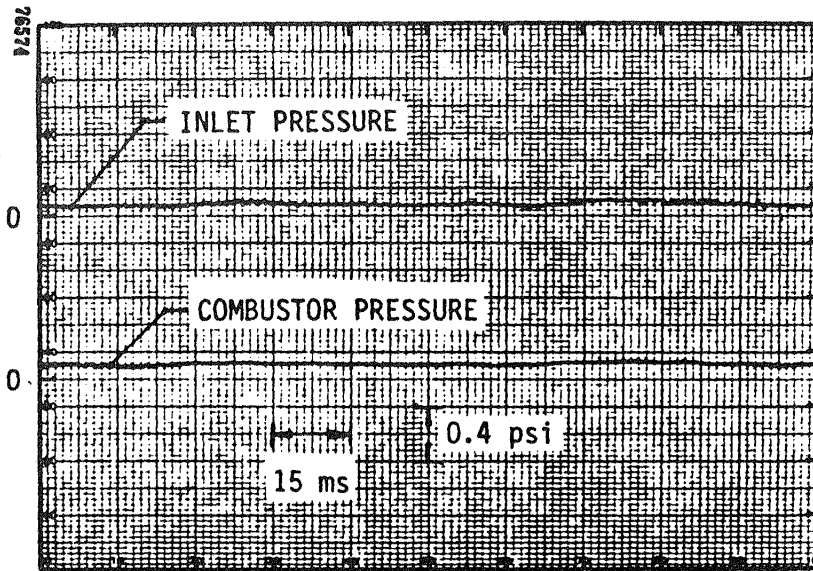


(c) Equivalence ratio, 0.506; flame flickering.

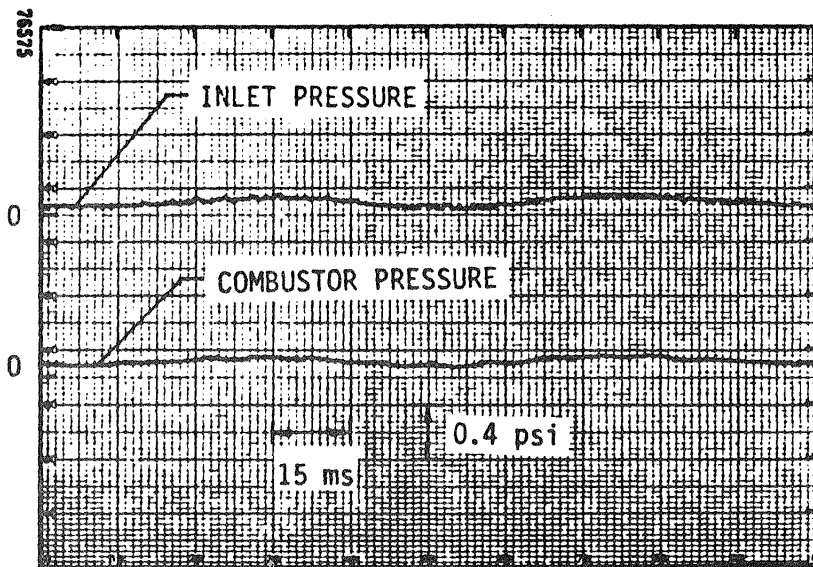


(d) Equivalence ratio, 0.74; flame stabilized in premixer.

Figure 19. Concluded.

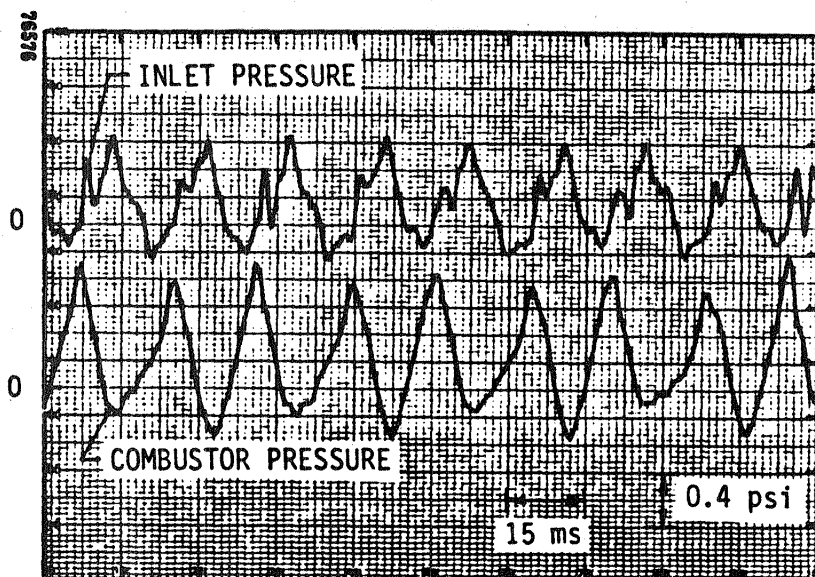


(a) Equivalence ratio, 0.373; lean flame in combustor, not at step.

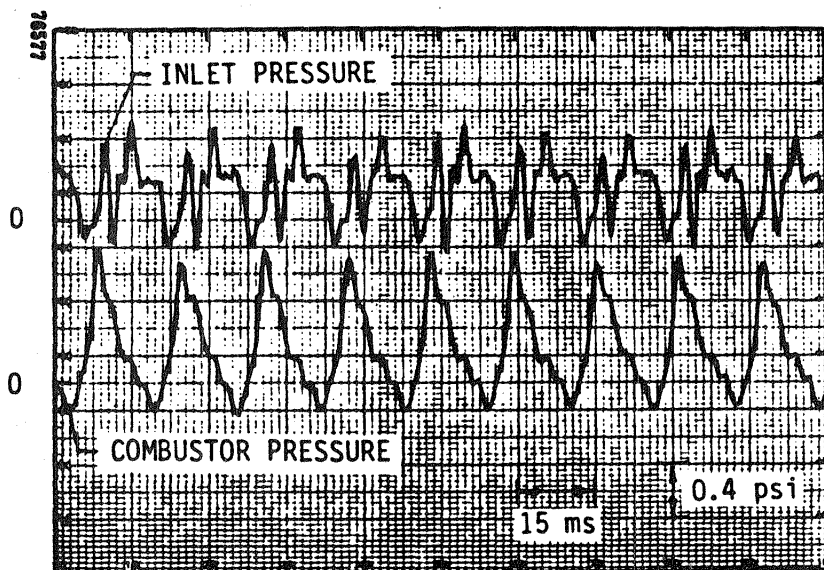


(b) Equivalence ratio, 0.387; lean flame at step.

Figure 20. Inlet and combustor pressure traces at inlet air temperature, 715K; premixer wall temperature, 700K; average premixer velocity, 60 ft/s; fuel injector 8in. upstream of step; pressure taps 43.75in. apart.

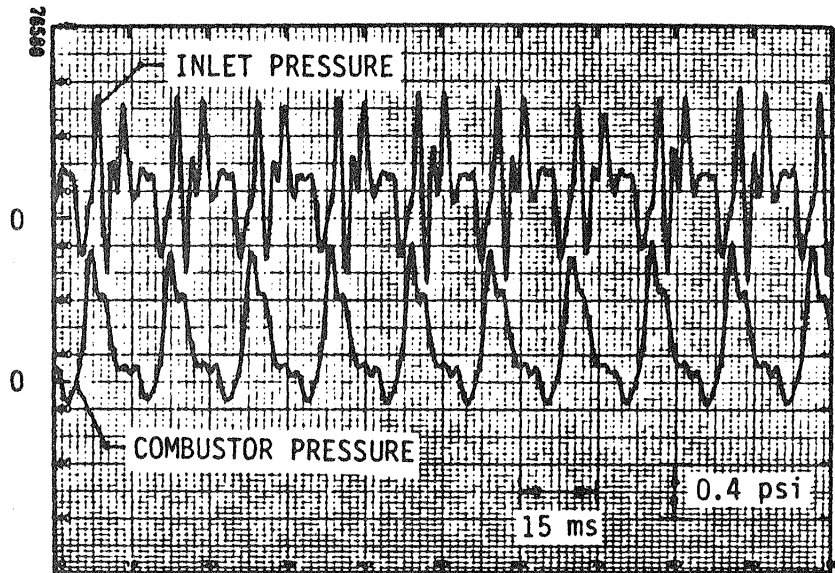


(c) Equivalence ratio, 0.415; flame flickering.

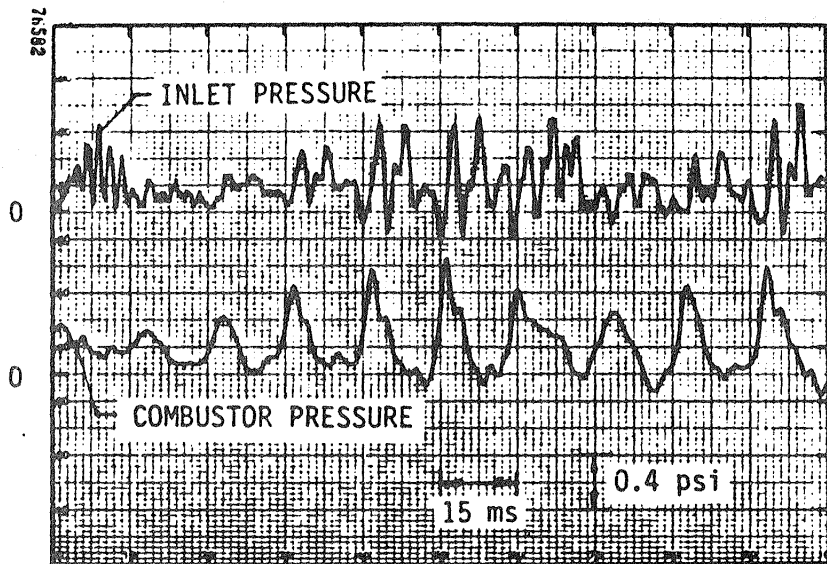


(d) Equivalence ratio, 0.480; flame flickering.

Figure 20. Continued.

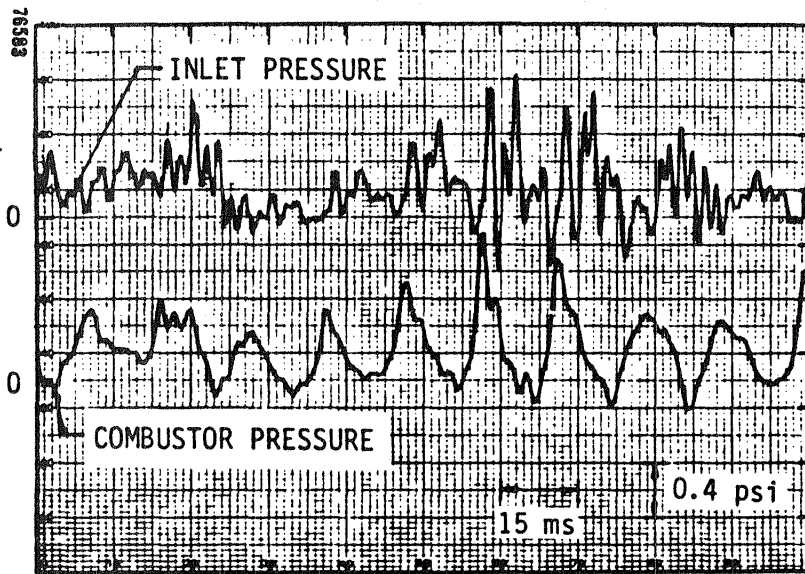


(e) Equivalence ratio, 0.567; flame flickering.



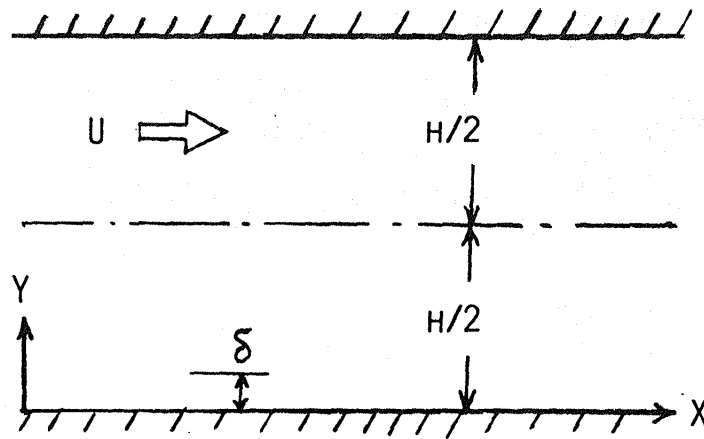
(f) Equivalence ratio, 0.637; momentary flashback.

Figure 20. Continued



(g) Equivalence ratio, 0.695; momentary flashback.

Figure 20. Concluded.



$$\delta = \sqrt{2\nu/\omega}$$

$\nu$  = Kinematic Viscosity of Air

$\omega$  = Oscillation Frequency in Radian/sec

Figure 21. Coordinates for the Periodic Flow Analysis in the Premixing Channel

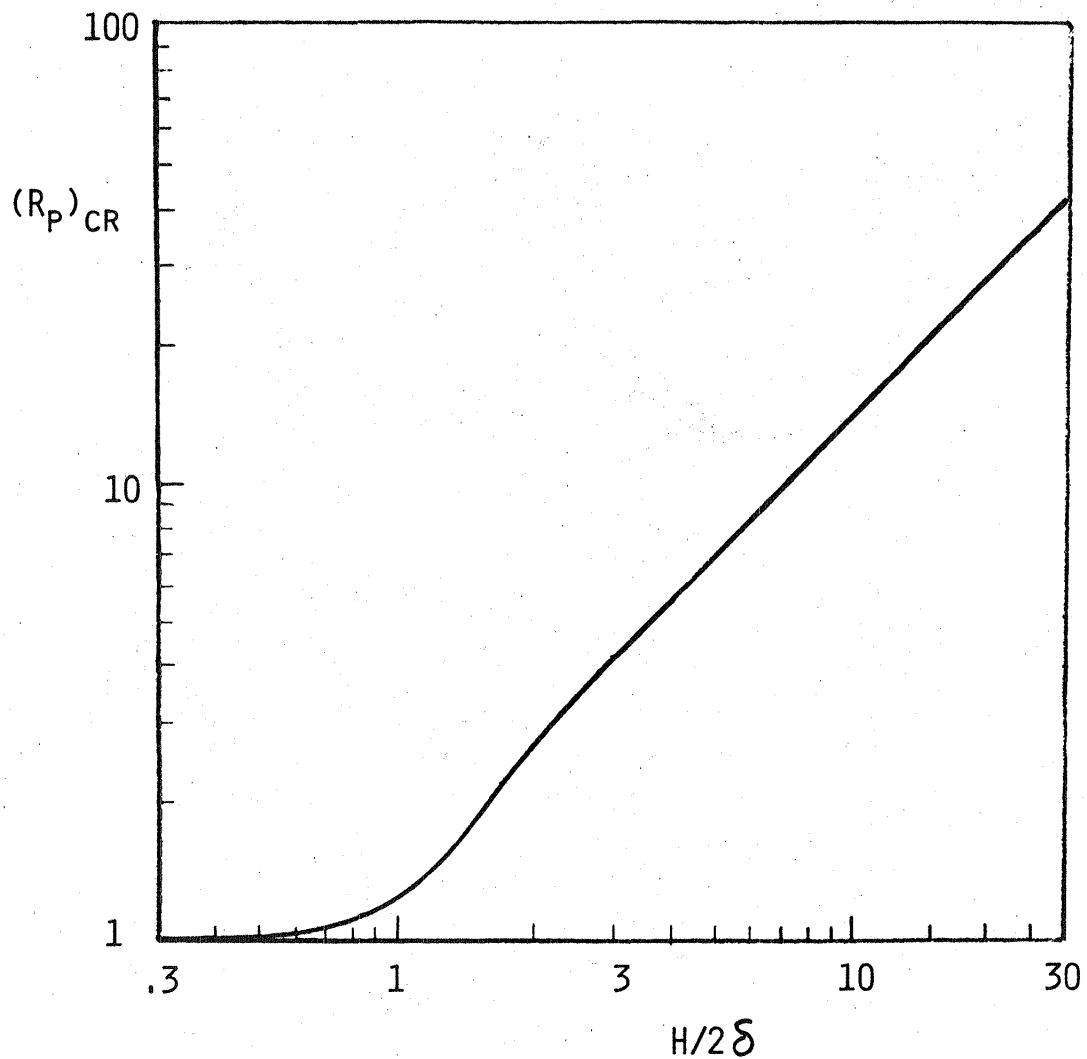


Figure 22. Critical Pressure Gradients Ratio for Flow Reversal vs. Ratio of Channel Half-height to Oscillation Characteristic Depth

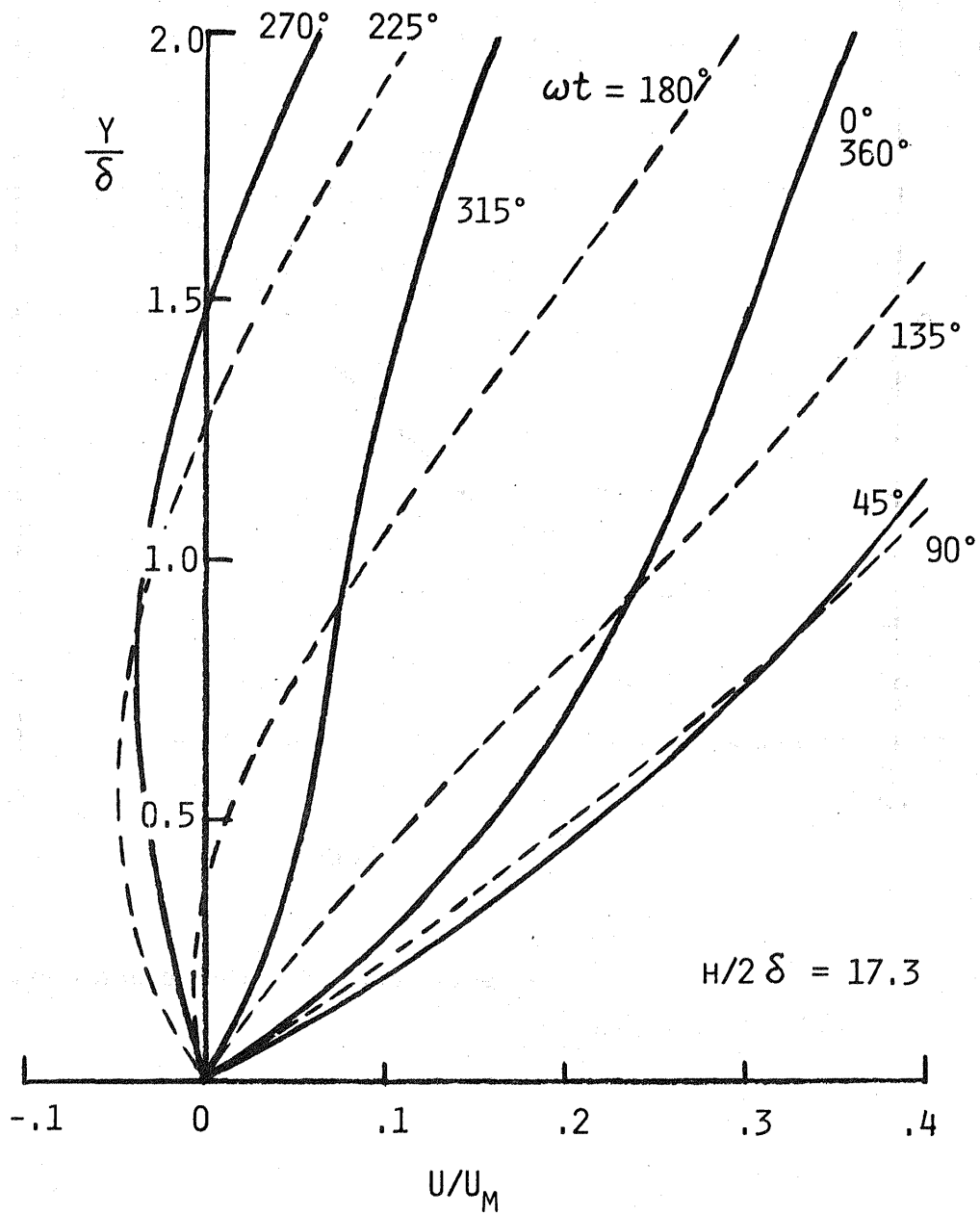


Figure 23. Near-Wall Velocity Profiles for  $r_p = 50$

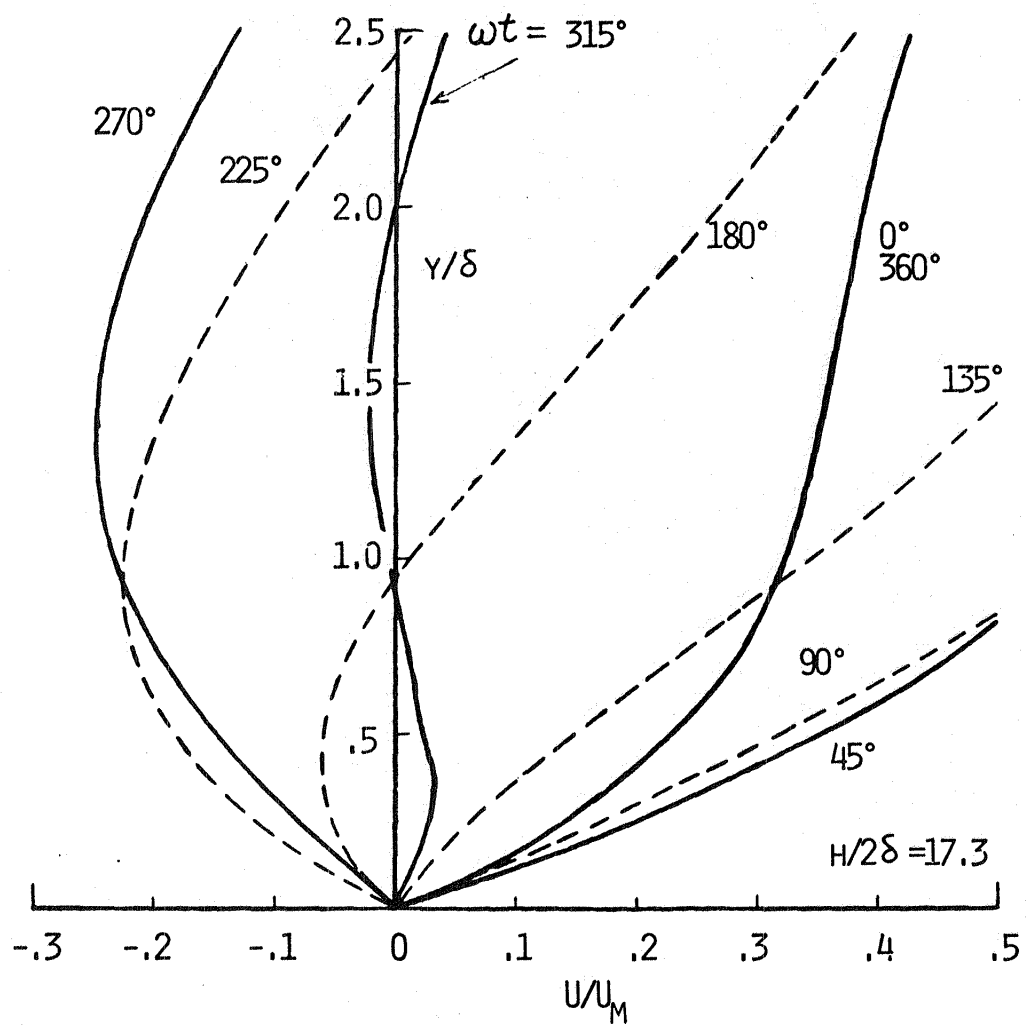


Figure 24. Near-Wall Velocity Profiles for  $r_p = 100$

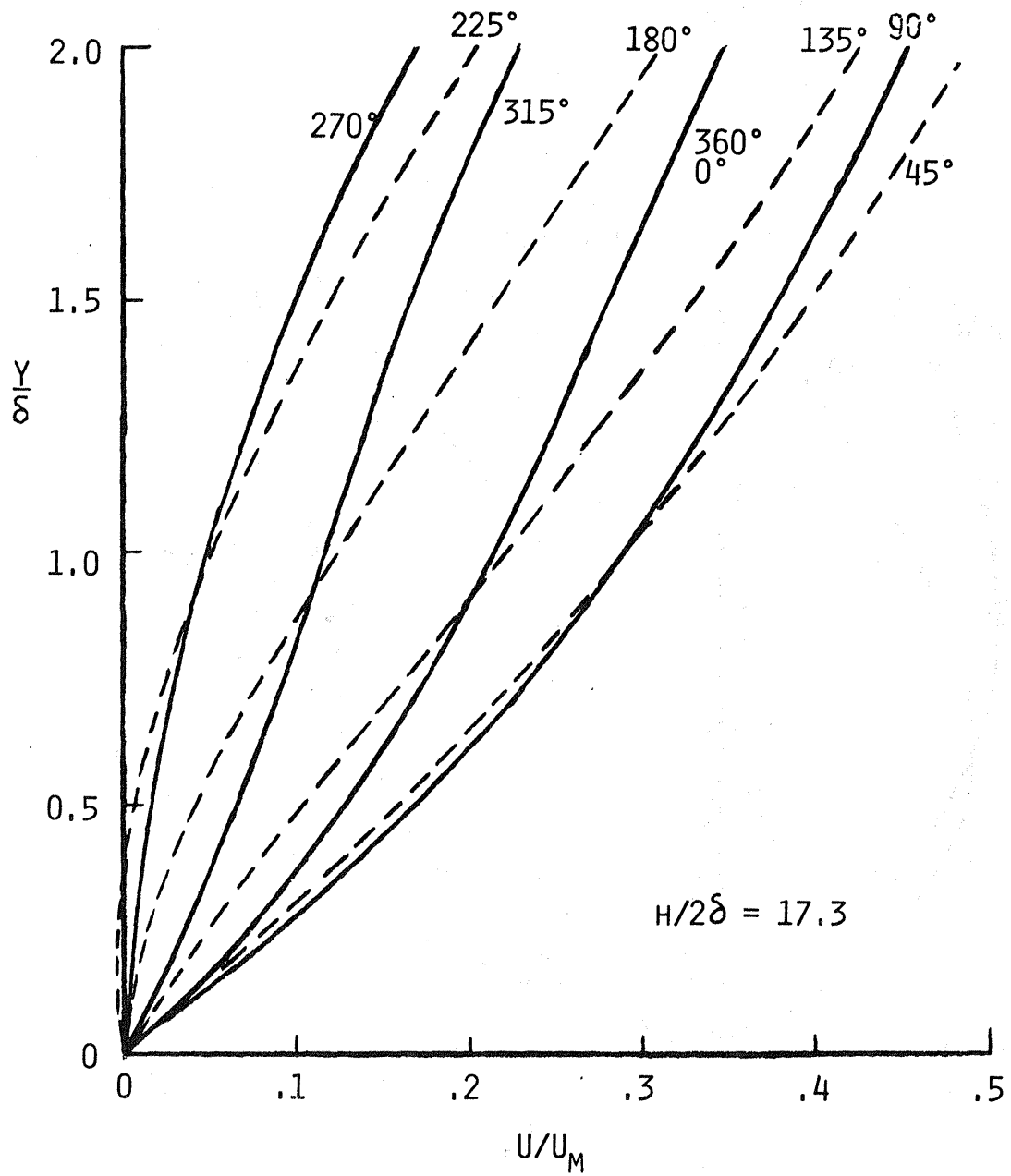


Figure 25. Near-Wall Velocity Profiles for  $r_p = 30$

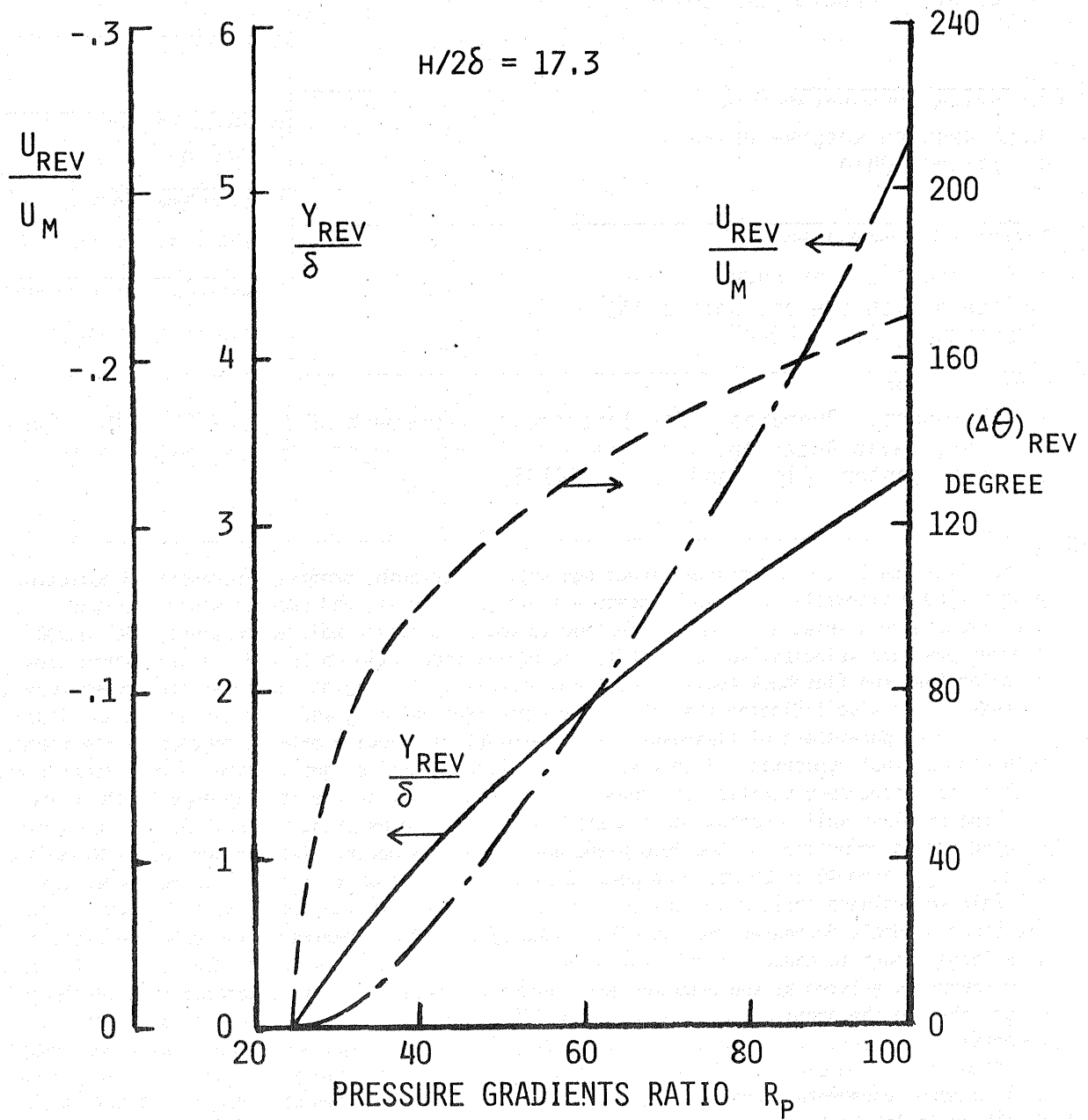


Figure 26. Maximum Reversal Velocity ( $u_{rev}/u_m$ ), Reversal Depth ( $y_{rev}/\delta$ ) and Duration of Flow Reversal ( $\Delta\theta_{rev}$ ) as a Function of Pressure Ratio  $r_p$ .

1. Report No. NASA CR-174961	2. Government Accession No.	3. Recipient's Catalog No.	
4. Title and Subtitle Combustor Flame Flashback		5. Report Date June 1985	
		6. Performing Organization Code	
7. Author(s) Margaret P. Proctor and James S. T'ien		8. Performing Organization Report No.	
		10. Work Unit No.	
9. Performing Organization Name and Address Case Western Reserve University Cleveland, Ohio		11. Contract or Grant No. NAG 3-290	
		13. Type of Report and Period Covered Contractor Report	
12. Sponsoring Agency Name and Address U.S. Department of Energy Office of Vehicle and Engine R&D Washington, D.C. 20545		14. Sponsoring Agency Code Report No. DOE/NASA/0290-1	
15. Supplementary Notes Final Report. Prepared under Interagency Agreement DE-AI01-77CS51040. Project Manager, David Anderson, Altitude Wind Tunnel Project Office, NASA Lewis Research Center, Cleveland, Ohio 44135.			
16. Abstract A stainless steel, two-dimensional (rectangular), center-dump, premixed-prevaporized combustor with quartz window sidewalls for visual access was designed, built, and used to study flashback. Test conditions were: inlet air temperature, 600 to 850 K; premixer wall temperature, 450 to 900 K; average premixer velocity, 40 to 80 ft/s; and equivalence ratio up to 0.8. A parametric study revealed that the flashback equivalence ratio decreased slightly as the inlet air temperature increased. It also indicated that the average premixer velocity and premixer wall temperature were not governing parameters of flashback. The steady-state velocity balance concept as the flashback mechanism was not supported. From visual observation several stages of burning were identified. High speed photography verified upstream flame propagation with the leading edge of the flame front near the premixer wall. Combustion instabilities (spontaneous pressure oscillations) were discovered during combustion at the dump plane and during flashback. The pressure oscillation frequency ranged from 40 to 80 Hz. The peak-to-peak amplitude (up to 1.4 psi) increased as the fuel/air equivalence ratio was increased attaining a maximum value just before flashback. The amplitude suddenly decreased when the flame stabilized in the premixer. The pressure oscillations were large enough to cause a local flow reversal. A simple test using ceramic fiber tufts indicated flow reversals existed at the premixer exit during flickering. It is suspected that flashback occurs through the premixer wall boundary layer flow reversal caused by combustion instability. A theoretical analysis of periodic flow in the premixing channel has been made. The theory supports the flow reversal mechanism. The question of why combustion instability occurs remains unclear. Until a more fundamental understanding is achieved on the mechanism of combustion oscillation, flame flashback is likely to be a potential problem with the premixed-prevaporized combustors.			
17. Key Words (Suggested by Author(s)) Combustion; Premixed flames; Flashback		18. Distribution Statement Unclassified - unlimited STAR Category 44 DOE Category UC-96	
19. Security Classif. (of this report) Unclassified	20. Security Classif. (of this page) Unclassified	21. No. of pages 80	22. Price* A05

**End of Document**